The Journal of

Cell Culture Models

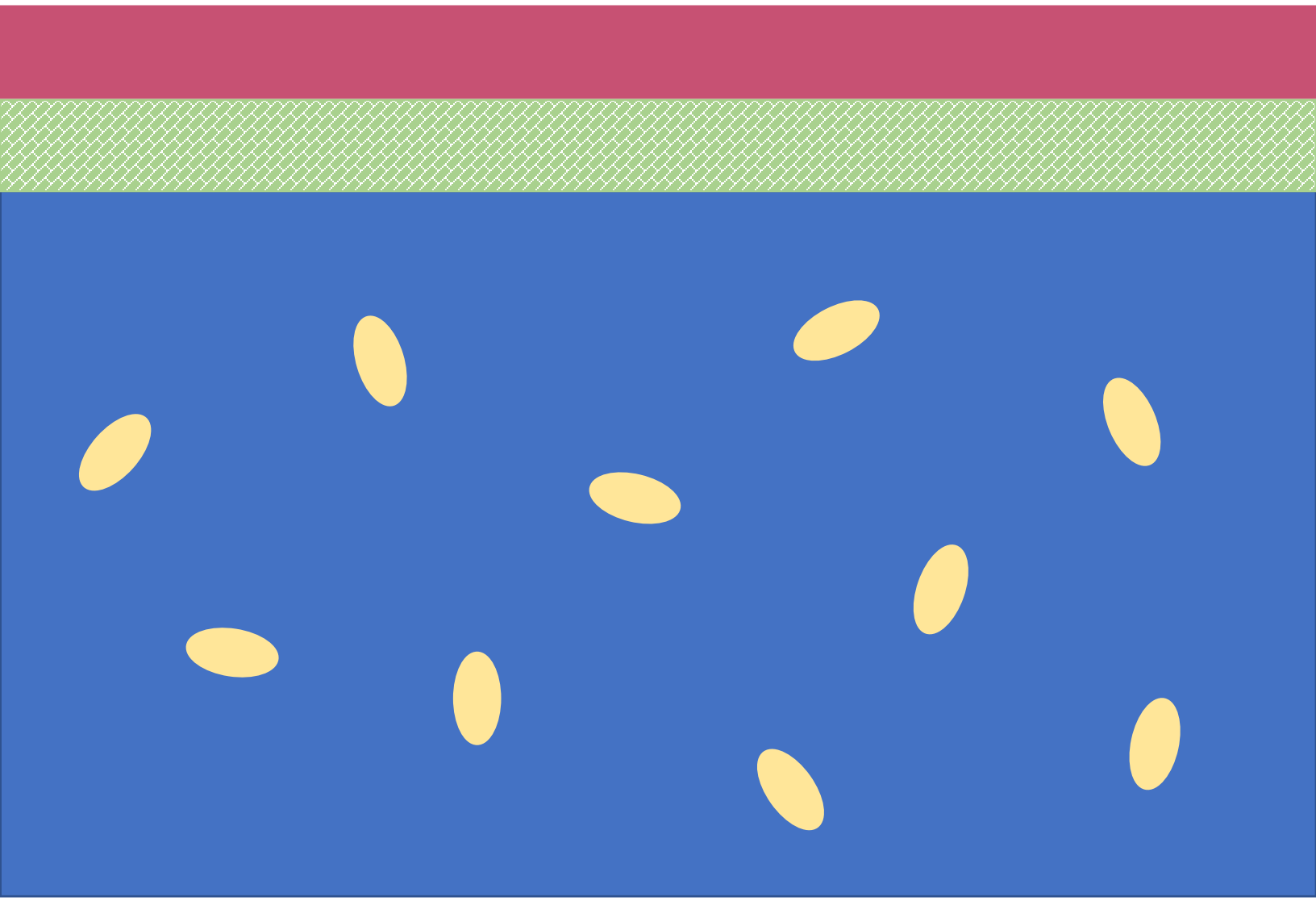

Cover art credit: Olivia Atkins

Edited by Louis A. Roberts

The Journal of Cell Culture Models

Louis A. Roberts

Worcester Polytechnic Institute

Worcester, MA

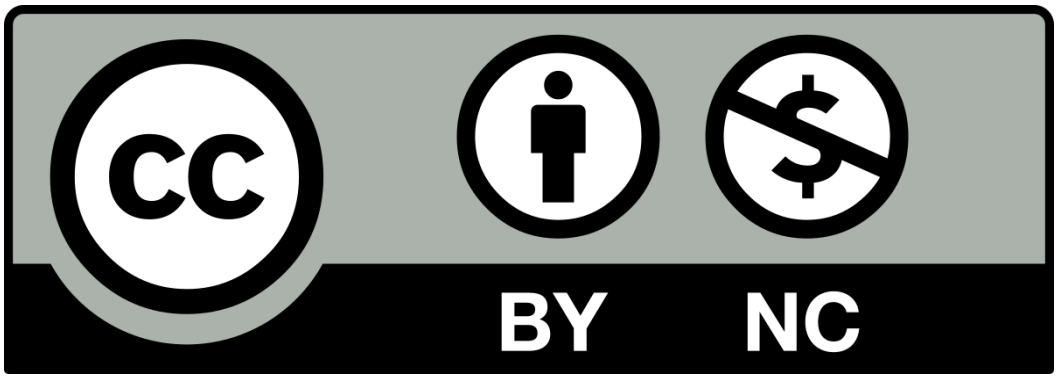

Collection Description

While often cells are represented and pictured as discrete biological units, we aim to expand our vision where cells are more realistically considered as building blocks of tissues. By focusing on their interactions with other cell types and biocompatible materials, we can better model the integrated nature and three-dimensional structures that inform cell survival, proliferation, differentiation, and biological function. This approach better allows us to understand the molecular and cellular processes that mediate and affect scarring, wound healing, drug toxicity, and cell development. How do cells choose between these outcomes, and how can different cell types and their interactions with materials direct these processes? Our biologically authentic cell culture models help answer these research questions with the goal of contributing to regenerative medicine applications.

This collection can be viewed as a "Journal of Cell Culture Models", and contains articles written following the processes and adhering to the conventions of the primary scientific literature. Each work herein was authored by undergraduate students at Worcester Polytechnic Institute (WPI) enrolled in an authentic research laboratory course, and credits the teaching assistant and instructor (as corresponding author). Generating and disseminating this collection was made possible via the generous support of the WPI Women's Impact Network (WIN) EmpOwER program. We especially acknowledge Lori Ostapowicz-Critz, George C. Gordon Library Associate Director - Scholarly Communication and Open Strategies for her expertise in assembling this open access journal.

Foreword for Volume II

This volume reflects the contributions of the students enrolled in the undergraduate laboratory course BB 3570 Cell Culture Models for Tissue Regeneration at Worcester Polytechnic Institute. The articles in this volume reflect a theme that emerged during the course- investigating the roles of cellular oxidative stress in injury, healing, and cancer. The students chose this theme as a way to study the models they designed, built, and tested. The student groups' findings are presented herein as an open-access journal article. While the research and writing are guided by the instructor and teaching assistant, the students are the scientists conceiving, executing, and disseminating their work. We are all proud of their creativity!

Volume II, 2024 contributors*

Sarah Aspinwall, Jamie Baines, Hayden Bovard, Tara Bromfeld, Samuel Levitan, William Miller, Sarah Oliveira, Nicole Rannikko, Theresa Rosato, Isabella Sheeran, Grace Solod, Ren Vitellaro, Miles Williams, Vanesa Lopa (teaching assistant), Shruti Shastry (teaching assistant), and Louis Roberts (instructor).

*We wish to acknowledge the research of three additional students (Trevor Bush, Joceyln Hinchcliffe, and Alana Lue Chee Lip). Their article is not included as it may contribute to a publication or patent.

Table of Contents

Antioxidant Effects of Blueberry-Rich Chitosan-Based Hydrogels on HaCaT Cells After UV Radiation

Tara Bromfield, Isabella Sheeran, Nicole Rannikko

[a] *Department of Biology and Biotechnology, Worcester Polytechnic University, Worcester, MA*

Students: tabromfield@wpi.edu*, nrannikko@wpi.edu, iesheeran@wip.edu Mentor: laroberts@wpi.edu

ABSTRACT

Reactive oxidative species (ROS) are molecules containing free radicals that are associated with adverse health effects such as DNA damage, modifications of genes or proteins, and more. ROS can also stimulate aging through the hyaluronidase enzyme, which destroys hyaluronic acid and lessens elastin and collagen fibers in the skin. Antioxidants containing high levels of polyphenols have been shown to reduce these free radicals, preventing some of these impacts and delaying skin aging (photoaging). Human keratinocytes are the most common cell type in the skin and can be evaluated for ROS damage in the epidermis layer. In this study, the antioxidant abilities of a chitosan hydrogel, enriched with blueberry extract, were investigated through *in vitro* studies with HaCaT keratinocyte cells. These cells were embedded in the hydrogel and exposed to UV radiation to induce ROS. Through the use of a DCFDA cellular ROS assay, the amount of ROS in cells treated with the extract versus cells without extract was investigated. At the conclusion of the study, it was determined that the hydrogel containing the extract and HaCaT cells showed no fluorescence above the background readings, while the cells embedded in the hydrogel without extract showed fluorescence ranging from 200-300nm. Therefore, the hydrogels containing the extract have fewer ROS species present compared to the hydrogel without the extract, implicating the extract's antioxidant and potential anti-aging properties. Future studies testing different amounts of UV radiation, higher concentrations of extract, and other cell types such as fibroblasts may reveal the extent of blueberry's antioxidant properties.

KEYWORDS

Reactive Oxygen Species, HaCaT cells, Blueberry Extract, Chitosan, Ultraviolet Radiation, Hydrogel, Antioxidant, Skin aging

INTRODUCTION

Reactive oxidative species (ROS) are molecules that contain unstable oxygen species that have at least one unpaired electron, also known as free radicals (Jakubczyk et. al., 2020). ROS is known to cause adverse health effects such as DNA damage, modifications of genes or proteins, and more. ROS can also stimulate the hyaluronidase enzyme, which destroys hyaluronic acid and lessens elastin and collagen fibers in the skin (Studzińska-Sroka et. al, 2024). Antioxidants are compounds that can scavenge these free radicals and prevent further damage that may occur in cells. Blueberries, or *Vaccinium cyanococcus,* are fruits characterized by having high levels of antioxidants. These antioxidants could help reduce damage caused by ROS in human skin cells. To investigate this, the HaCaT cell line was utilized.

The HaCaT cell line is derived from adult human keratinocytes, or skin cells. Keratinocytes make up the major cell type of the epidermis, or the outermost layer of the skin (Pastar et al., 2014). Under a microscope, these cells can be identified as nucleus free, flat, squamous cells with high concentrations of keratin. They are created in the stratum basale layer, or the deepest layer of the epidermis, and migrate to the stratum corneum. The HaCaT cell line is a non-tumorigenic monoclonal cell line that proliferates well in traditional media

(Deyrieux et al., 2007) and can have a long lifespan without a feed layer or additional growth factors (Colombo et al., 2017), Overall, HaCaT cells function to form the protective layer of the body, blocking foreign substances, and conducting the wound healing process (Pastar et al., 2014). They keep in heat, moisture, and other important nutrients, while also bonding with other cells in the epidermis. They can be made into 2D or 3D cultures, stemming from a single donor or multiple pooled donors ("Keratinocytes", n.d.). The versatile and adaptive nature of HaCaT cells makes them useful in understanding the largest organ in the body, our skin.

When building a cell culture model, biomaterials can provide more realistic and effective in vitro studies of mammalian cells. Chitosan, a biopolymer discovered by Charles Rouget in 1859, is a commonly engineered biomaterial (Cato et al, 2014). There was a lack of interest in this biomaterial because of its rigid structure and resistance to common solvents, compared to cellulose, another compound of similar structure. Today, chitosan is being researched as a biomaterial for tissue engineering. This natural biomaterial is a great source to use because of its biocompatibility, biodegradability, antimicrobial properties, and functionality (Cato et al, 2014). The properties of chitosan rely on molecular weight and deacetylation (DDA) and is commonly found in crustaceans (Cato et al, 2014). At warmer conditions, this biopolymer is very adaptable, as it can take on different forms due to its solubility in dilute acid solutions (Cato et al, 2014). It is a great biomaterial for carrying proteins and other active molecules because of the cations of the molecules and the functional amine and hydroxyl groups on molecular chains (Cato et al, 2014). Due to its antimicrobial properties, ability to form a hydrogel in dilute acids, and affinity for carrying active molecules, chitosan hydrogel was chosen as the primary delivery method of the blueberry extract in the assays conducted.

Photoaging, or the process of skin aging due to UV radiation from the sun, is often linked to reactive oxidative species (ROS) resulting from the radiation. Substances containing high levels of antioxidants and polyphenols have been shown to reduce these free radicals, preventing some of these impacts and delaying skin aging, or loss of collagen. A recently published article detailed the use of bilberry-fruit extract in chitosan-based hydrogels for its anti-aging properties (Studzińska-Sroka et. al, 2024). Biologically active extracts from *Vaccinium myrtillus* and *Vaccinium corymbosum* (bilberry and blueberry) were tested to determine their antioxidant properties. These extracts were then used in an MTT assay to test their cytotoxicity on HaCaT keratinocytes, which was determined to be very low. Chitosan hydrogels were created using the bilberry extract based on the results of the antioxidant and MTT assays (Studzińska-Sroka et. al, 2024). These hydrogels were shown to have many antioxidant and anti-aging properties, showing potential for future pharmaceutical use.

The protective properties of blueberry extract against UV radiation needs further exploration. While the extract-rich hydrogel was shown to have certain antioxidant properties, its ability to protect cells *in vitro* against UV-radiation has not been thoroughly explored. This paper begins to explore this area by investigating the ability of a *Vaccinium cyanococcus*-rich chitosan-based hydrogel to protect cells against UV damage. In this study, testing was completed to examine the amount of reactive oxidative species (ROS) present in human keratinocytes (HaCaTs) after UV radiation. One group of HaCaT cells was embedded in a blueberry extract-rich chitosan hydrogel while another group was embedded in a hydrogel without extract, acting as a negative control. This allowed for the investigation into the antioxidant and anti-aging properties of *Vaccinium cyanococcus.*

METHODS AND PROCEDURES

Cell Culture Techniques

HaCaT cells (AddexBio, Catalog No. T002001) were obtained and maintained in a complete medium solution made up of Dulbecco's Modified Eagle Medium (DMEM) (Corning, Catalog No. 10-013-CV), 10% Fetal Bovine Serum (FBS), and 1x penicillin-streptomycin. They were cultured in an incubator at 37°C with 5% CO_2 concentration. Cells were passaged about every 48 hours in new media.

Extract Preparation

Dried *Vaccinium Cyanococcus* fruit was bought online from the brand Pure Original Ingredients. 0.2g of the dried powder was weighed and added to a tube with 5mL of a 1:1 water and acetone solution. The tube was warmed in a 40°C water bath for 10 minutes. Every 10

minutes, 5mL more of the water-acetone solution was added. These steps were conducted a total of 4 times, with 20mL of solution as the final volume. The extract was centrifuged at 3000 rpm for 5 minutes until a pellet of the dried powder formed at the bottom of the tube. The extract was decanted from this tube and 5mL of the extract was placed in 4 separate tubes, each. These tubes were left in a sterile biological hood for 48 hours to evaporate the acetone from the extract. The remaining solution was then put through a sterile vacuum filtration process to ensure sterility before being replenished with complete medium to its previous volume and 1% concentration.

Hydrogel Preparation

A 3% chitosan hydrogel in 1% acetic acid was obtained from a previous study (Papi et. al., 2021). In the original study, the hydrogel was prepared by dissolving 3g of chitosan (Sigma-Aldrich, Product No. 448869-50G) in 100 mL of 1% acetic acid and stirring the solution for 24 hours until a gel-like substance formed (Papi et. al, 2021). The hydrogel primarily used in this study contained 1.5% chitosan, which was prepared by mixing the 3% chitosan with equal amounts of 1% acetic acid.

Embedding Cells in Hydrogel

Initial testing was conducted to determine the best composition of a chitosan hydrogel for cell growth. Cells were embedded in both 3% and 1.5% chitosan hydrogels to qualitatively determine their effect on HaCaT cell growth. HaCaT cells were first removed from a T-75 plate by trypsinization and counted using a cellometer. After cell counting, it was determined that the cells would be plated with either 100,000 or 50,000 total cells per well. Equal volumes of cells in media and chitosan hydrogel were mixed in 15mL conical tubes before plating. The solutions were then plated in a 6-well plate as shown in Figure 1 below, with a total volume of 1.5mL per well. 1.5mL of additional complete medium was added to the top of each well before the plate was placed in an incubator at 37℃ with 5% CO2 concentration for 72 hours. The wells were then observed and qualitatively analyzed to determine which hydrogel composition and seeding concentration yielded confluent wells after incubation.

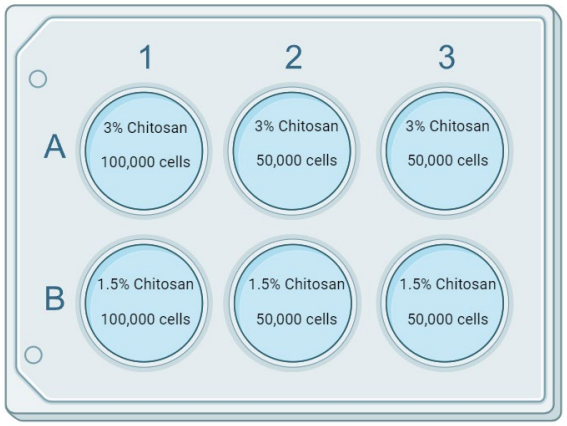

Figure 1: Plate Set-up for Initial Embedding of Cells in Different Compositions of a Chitosan Hydrogel.

After initial testing was completed and the best hydrogel concentration was determined, additional HaCaT cells were plated in 6-well plates for future assays. To prepare the cells, the cell count was determined in a confluent T-75 plate using a cellometer. The cells were trypsinized and placed in fresh media before being counted. Four million HaCat cells were present in the T75 flask and therefore 500,000 cells per were plated, per well, for two six-well plates. Separate hydrogel mixtures were created for the extract-containing wells and the wells without any extract in two different 15mL conical tubes. 3mL of 1.5% chitosan was added to each tube. 3mL of complete media containing $2x\ 10^5$ cells were also added to each tube. In one tube, 2mL of 1% extract was added (500ul of extract per well). In the other tube, 2mL of complete media was added to keep the total volumes consistent. The solutions were then plated in 2 wells of a 6-well plate, with 2mL of the solutions per well. Two wells of each solution were filled per plate as technical replicates. The last 2-wells of the plate were filled with 2mL of just 1.5% chitosan to visually compare the matrix structure. A diagram of the set-up can be seen in Figure 2. After all of the hydrogels were plated, 2mL of media was added to the top of the gel and the plates were placed in an incubator at 37 ℃ for 24 hours before UV radiation.

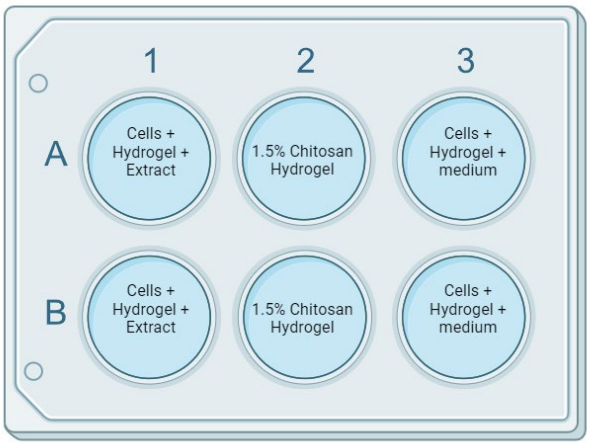

Figure 2: Plate Set-up for Treated and Untreated Cells Before UV Radiation.

UV Radiation Treatment

The plates were treated with UV radiation from the germicidal light (30W, UVC 254nm) of the cell culture hood. The first 6-well plate was placed under the UV light for 2 hours. The second plate was placed under the light for 1 hour. After both plates had undergone the treatment, they were placed back in the incubator for 24 hours. The amount of UV radiation to induce sufficient ROS in the HaCaT cells was unknown, therefore 1 hour and 2 hours were tested. It was noted that after only 1 hour of UV radiation, moat samples did not contain fluorescent values greater than background fluorescence, indicating that there was very little ROS induced in those cells. Therefore, only data from the 2-hour trials were considered for further analysis.

DCFDA Cellular ROS Assay

Reactive oxidative species levels were detected in the HaCaT cells after UV radiation through the use of a DCFDA (2'7' dichlorodihydrofluorescein diacetate) cellular ROS assay (Sigma Aldrich, Product No. D6883). To remove the cells from the hydrogel, the chitosan was degraded using 2mL of 1% acetic acid in each well of the two 6-well plates. The acid was allowed to sit in the wells for 5 minutes before the solutions were transferred into 8 distinct 15 mL conical tubes. The wells were rinsed by adding PBS and scraping the bottom of the wells to ensure all cells were transferred to the conical tubes. The conical tubes were then centrifuged for 5 minutes, or until a pellet formed at the bottom of each tube. The chitosan solution was aspirated off the top of the pellet, after which 4mL of PBS was added to the tubes. The pellet was dispersed by pipetting and the tubes were centrifuged again. The PBS was aspirated off and 0.8mL of diluted DCFDA solution (10uL of DCFDA, 5 mL of PBS, 5 mL of complete media) was added to each sample to give a concentration of $1x\ 10^6$ cells/mL in each tube. The tubes were placed in a 37 ℃ incubator for 72 hours to allow the cells to become stained. The tubes were then centrifuged once again and the cells were washed once with PBS. The cells were then resuspended in 0.8mL of PBS before being plated in a black walled 96-well plate. 0.1mL of solution was added to 64 wells of the 96-well plate to have a concentration of 100,000 cells/well. The plate was then placed into a fluorescent plate reader, which was set to emit 485 nm/535 nm. The RFUs for each well were recorded.

RESULTS

Cell Embedding Test

Two concentrations of chitosan were evaluated for cell growth in the hydrogel, 3% chitosan and 1.5% chitosan. Ultimately, the HaCaT cells were more confluent and showed healthier cell morphology when embedded in the 1.5% chitosan hydrogel when compared to the 3% hydrogel, as shown in Figure 3 below. Therefore, further experiments were conducted with the 1.5% chitosan hydrogel. The wells with 100,000 cells were also shown to be much more confluent, without overcrowding, than the wells plated with 50,000 cells. However, the cells were not nearly as confluent as hoped after 48 hours. Therefore, the cell seeding density was increased to 500,000 cells per well for future assays. This would allow for there to be almost a million cells in each well after incubation. After 48 hours, it was qualitatively estimated that there were around 800,00 cells per well. This lower growth rate may have been due to HaCaT cells naturally having a slower doubling time and the hydrogel matrix impacting the interaction between the cells and the media.

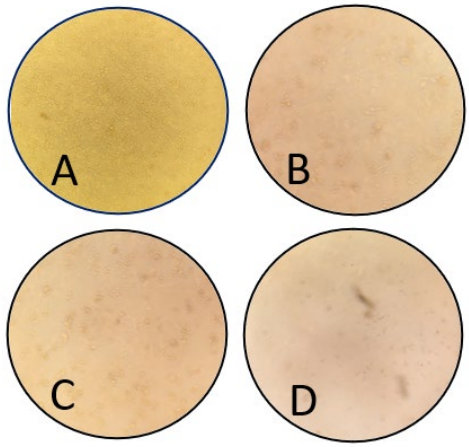

Figure 3: Microscope images of HaCaT cells embedded in chitosan hydrogel at 100X magnification. Image A displays 100,000 cells embedded in a 1.5% chitosan hydrogel. Image B displays 100,000 cells embedded in a 3% chitosan hydrogel. Image C displays 50,000 cells embedded in a 1.5% chitosan hydrogel. Image D displays 50,000 cells embedded in a 3% chitosan hydrogel.

DCFDA Cellular ROS Assay

The fluorescent data from the DCFDA cellular ROS assay showed that the HaCaT cells treated with the blueberry extract had less ROS than cells that were untreated after 2 hours of UV radiation (Figure 4). The treated cells all had RFUs at or below background fluorescence, while the untreated cells had RFUs ranging from 200-300nm after accounting for background, as displayed in Table 1 below. Our hypothesis for this experiment was that blueberry extract would cause a decrease in ROS in HaCat cells after UV radiation due to the fruit's antioxidant properties. Our results support this hypothesis and show that when HaCat cells are placed under UV radiation for at least two hours, blueberry extract can help protect the cells from UV damage. As mentioned in the methods section above, the majority of the cells exposed to 1 hour of UV radiation did not show RFUs higher than background fluorescence. Therefore, it was concluded that the HaCaT cells require at least 2 hours of UV exposure to induce sufficient ROS for comparison between treatments. Only the data from the cells exposed for 2 hours was further analyzed.

Table 1: Results from the ROS Detection Assay for treated and untreated HaCaT cells exposed to 2 hours of UV radiation.

Extract	RFUs								Avg.	St. Dev
+	0	0	0	0	0	0	0	0	0	0
+	0	0	0	0	0	0	0	0	0	0
-	282	248	271	235	209	255	274	297	258.9	26.4
-	216	259	229	177	193	203	220	224	215.1	24.8

The table above shows the RFU values from the ROS detection assay of the treated and untreated HaCaT cells after UV radiation. The E rows represent the samples treated with extract and the NE rows represent the untreated samples without extract. The four rows display the values from the two technical replicates of each condition (+/- extract). The columns represent the individual wells of the 96-well plate that were read. The 0 values represent RFUs that were at or below background fluorescence.

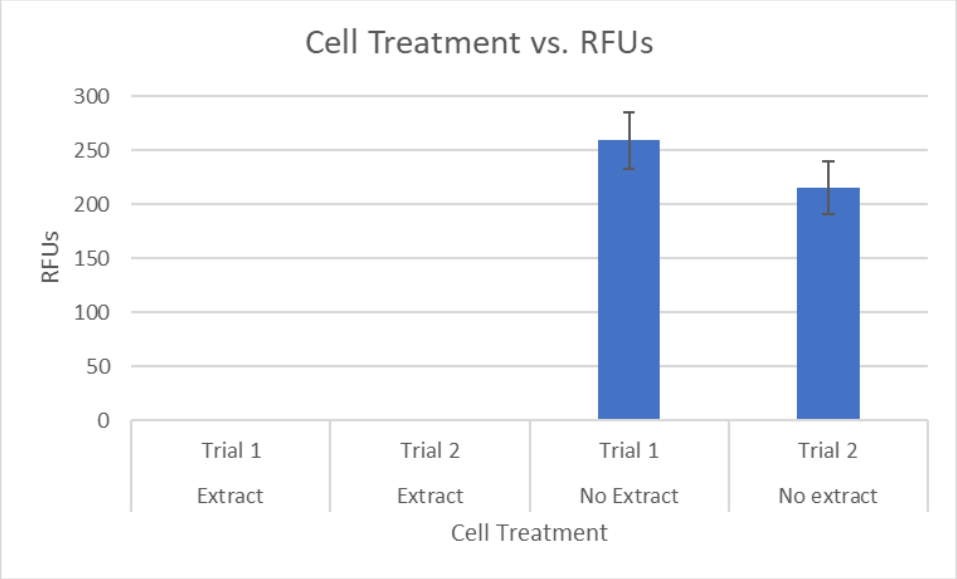

Figure 4: RFUs for Treated and Untreated HaCaT cells exposed to 2 Hours of UV Radiation. The "extract" label indicates that the cells were treated with the blueberry extract while the "no extract" label indicates the cells were not treated with the extract. The graph displays the average RFUs for each trial. The graph shows that the trials with extract showed no fluorescence above the background while the trials without extract showed fluorescence between 200-300 RFUs. The error bars represent the standard deviation from each trial.

DISCUSSION

Based on the experiments performed, it was determined that blueberry extract can protect HaCaT cells by reducing ROS induced by UV radiation. Our findings are consistent with previous studies that have investigated the biological characteristics of blueberries. It has been shown that blueberries contain high levels of polyphenols flavonoids and anti-hyaluronidase and anti-tyrosinase properties that can protect against photoaging (Studzińska-Sroka et. al, 2024). Chitosan also contains anti-inflammatory and antioxidant properties, making it an ideal delivery method for the extract. When UV radiation is absorbed by the skin, ROS species increase in skin cells leading to decreasing skin elasticity and firmness. Having these antioxidant and protective properties may help delay the negative effects of photoaging, implicating the potential pharmaceutical uses for blueberry extracts.

All final hydrogels were created with a concentration of 1.5% chitosan. As mentioned above, this solution was prepared by mixing equal parts of a 3% chitosan solution and 1.0% acetic acid. Chitosan concentrations significantly impact anti-hyaluronidase activity, anti-tyrosinase activity, and the rate of cell proliferation, therefore our team had to carefully choose a reasonable concentration. Higher concentrations of chitosan increase the viscosity of the gel and therefore cause a slower release of compounds (Studzińska-Sroka et. al, 2024). Chitosan's naturally thick viscosity can slow the rate of cell proliferation as chitosan interacts with polymer surface topography, altering cell behavior and slowing cell growth (Martín-López et al., 2013). A low concentration would allow consistent and quick release of the extract's antioxidant compounds, which led to our choice to use 1.5% chitosan for the final assay.

Further testing into the properties of *Vaccinium cyanococcus* extracts should be completed. The experiment above only tests a 1% extract solution, but it would be beneficial to understand the effects of higher extract concentrations on HaCaT cells. In addition, a cell viability assay should be done, especially if testing different chitosan concentrations. This would present quantitative results regarding cell proliferation and display if higher concentrations were affecting cell growth. A total protein assay could also be used to evaluate the total number of proteins in each well, which impacts the fluorescence and ROS. Our group found that some variability in technical replicates, and a total protein assay would help reveal if the cells were consistently transferred to the 96 well plate. This would ensure there is a consistent number of proteins in each well. Furthermore, the effects of UV radiation should be evaluated at multiple time increments of longer duration and at different wavelengths. We only tested one and two hours (the one-hour results were inconclusive) but longer durations could show more of an effect on the HaCaT cells. Lastly, due to the highly viscous nature of chitosan, seeding the HaCaT cells at a higher density could help with achieving a higher confluency for more accurate assays.

CONCLUSIONS

At the conclusion of the study, testing showed that HaCaT cells treated with a *Vaccinium cyanococcus* extract showed a decrease in reactive oxidative species (ROS) after two hours of UV radiation compared to untreated cells. Past studies have examined the effects of extracts high in polyphenols on HaCaT cells, but our research was the first assay to test the impact of blueberry extract on UV radiation damage. Our results support the potential of blueberry extracts in skin care or other pharmaceutical and topical applications. Future studies could continue this research by utilizing varying concentrations of blueberry extract, testing other assays to obtain more quantitative results, and increasing the duration of UV exposure to further investigate the antioxidant and anti-aging properties of *Vaccinium cyanococcus*.

ACKNOWLEDGMENTS

The authors thank Professor Lou Roberts, and teaching assistants Vanesa Lopa and Shruti Shastry for their continuous guidance and support with our research in Cell Culture Models for Tissue Regeneration.

REFERENCES

1. Jakubczyk, K., Dec, K., Kałduńska, J., Kawczuga, D., Kochman, J., & Janda, K. (2020). Reactive oxygen species—Sources, functions, oxidative damage. Polski Merkuriusz Lekarski: Organ Polskiego Towarzystwa Lekarskiego, 48(284), 124–127.

2. Studzińska-Sroka, E., Pczkowska-Walendowska, M., Erdem, C., Paluszczak, J., Kleszcz, R., Hoszman-Kulisz, M., & Cielecka-Piontek, J. (2024). Anti-Aging Properties of Chitosan-Based Hydrogels Rich in Bilberry Fruit Extract. *Antioxidants*, *13*(1), Article 1. https://doi.org/10.3390/antiox13010105

3. Pastar, I., Stojadinovic, O., Yin, N. C., Ramirez, H., Nusbaum, A. G., Sawaya, A., Patel, S. B., Khalid, L., Isseroff, R. R., & Tomic-Canic, M. (2014). Epithelialization in Wound Healing: A Comprehensive Review. *Advances in Wound Care*, *3*(7), 445–464. https://doi.org/10.1089/wound.2013.0473

4. Deyrieux, A. F., & Wilson, V. G. (2007, June 30). *In vitro culture conditions to study keratinocyte differentiation using the HaCaT cell line - cytotechnology*. SpringerLink. https://link.springer.com/article/10.1007/s10616-007-9076-1

5. Colombo, I., Sangiovanni, E., Maggio, R., Mattozzi, C., Zava, S., Corbett, Y., Fumagalli, M., Carlino, C., Corsetto, P. A., Scaccabarozzi, D., Calvieri, S., Gismondi, A., Taramelli, D., & Dell'Agli, M. (2017, December 17). *HaCaT cells as a reliable in vitro differentiation model to dissect the inflammatory/repair response of human keratinocytes*. Mediators of Inflammation. https://www.hindawi.com/journals/mi/2017/7435621/

6. *Keratinocytes*. PromoCell. (n.d.). https://promocell.com/cell-culture-basics/keratinocytes/

7. Cato T. Laurencin, Roshan James, Sangamesh G. Kumbar, Tao Jiang, (2014) *Chapter 5 - Chitosan as a Biomaterial: Structure, Properties, and Applications in Tissue Engineering and Drug Delivery*, 91-113, ISBN9780123969835, https://doi.org/10.1016/B978-0-12-396983-5.00005-3.

8. Papi, A., Wall, A., Kola, M. (2021). MCF7 and MEF Proliferation on Chitosan-Silkworm Silk Scaffolding: Analyzing potential research and wound healing applications. *Worcester Polytechnic Institute.*

9. Martín-López, E., Nieto-Díaz, M., & Nieto-Sampedro, M. (2013). Influence of chitosan concentration on cell viability and proliferation in vitro by changing film topography. *Journal of Applied Biomaterials & Functional Materials*, *11*(3), e151-158. https://doi.org/10.5301/JABFM.2012.10449

Promotion of Wound Healing of NIH-3T3 and HaCaT By Treatment of Elderberry or Rosehip Extract

*Sarah Aspinwall[a], Sarah Oliveira[a], Miles Williams[a]& Louis Roberts[*a]*

[a]Department of Biology and Biotechnology, Worcester Polytechnic Institute, Worcester, MA

https://doi.org/10.33697/ajur.2020.NNN

Students: sjaspinwall@wpi.edu,scoliveira@wpi.edu,mewilliams2@wpi.edu
*Mentor: laroberts@wpi.edu**

ABSTRACT

Sambucus nigra L. commonly known as elderberry and the rosehip plants of the Rosa species are both prominent holistic remedies that have traditionally been used for their wound healing properties. This work intends to investigate the purported therapeutic properties of both plants when applied to a burn wound inflicted on a monolayer of cells grown over collagen gel. This was measured through a wound healing assay which counted the number of cells that migrated into the burn wound after treatment, and an ELISA assay which was used to measure the levels of tumor necrosis factor-alpha (TNF-α), a biomarker with increased levels in burn victims. These methods measured the severity of the burn and therefore the effectiveness of the treatments in promoting wound healing. The wound healing assay suggested that cells treated with elderberry extract demonstrated a similar level of migration to non-treated cells, while cells treated with rosehip extract had a greatly increased level of migration compared to cells that underwent any other treatment. The ELISA assay indicates that TNF-α levels decreased steadily post-burn in cells treated with rosehip, and decreased then sharply increased in cells treated with elderberry. This suggests that rosehip extract had a positive impact on burn healing as decreasing levels of TNF-α indicates decreasing burn severity. While this data is limited due to complications and time restraints it does indicate that rosehip extract possesses a level of healing properties and could potentially be used to therapeutic effect in the future.

KEYWORDS

HaCaT; NIH-3T3; Wound Healing; TNF-alpha; Elderberry; Rosehip, ELISA

INTRODUCTION

A large amount of cell culture research is dedicated to advancing wound healing medicine and techniques. Cell culture research is particularly relevant to wound healing because it provides a controlled environment to study the underlying mechanisms behind tissue repair and regeneration. Relevant cell types such as fibroblasts and keratinocytes can be tested to simulate actual wound healing for this research. Many insights gained from cell culture research have contributed to the development of more effective wound-healing strategies, improving victim outcomes and quality of life. Additionally, holistic medicines have gained popularity as alternative methods of treatment, as the integration of holistic medicine with conventional wound healing treatments has shown promise. This experiment is relevant because it tests the actual wound-healing properties of two of these holistic treatments using cell culture techniques. The research question guiding this project is how TNFa production in human epithelial and fibroblast cells will be when the cells are inflicted with a burn wound and then treated with elderberry and rosehip extract. This allows us to quantify how rosehip and elderberry affect wound healing. Since TNFa is a biomarker that indicates cell damage, cells that are more damaged, therefore less healed, will have higher levels of the cytokine. Through this method, we will test how extracts made from elderberry and rosehip affect the healing properties of cells that have suffered a burn wound.

HaCaT cells are keratinocytes derived from a white adult man and are the epidermis's primary cells. The cells are aneuploidy, meaning they have a mutation that causes an incorrect number of chromosomes. Studies show that HaCaT cells can have 42 to 74 chromosomes present, specifically, the cells exhibit basal cell properties and exhibit mutations in both alleles of p53 which can explain the reason that the cells spontaneously transformed from normal skin in vitro (Pavez Lorie et al, 2020).Typical culture conditions include DMEM with 10% fetal bovine serum, calcium content in the medium causes HaCaT cells to have a partially or fully differentiated phenotype. The cells are attachment-dependent and grow as a monolayer on the plate. The cells tend to grow in small clumps until 100% confluency is met but lack uniformity in size. Each cell is only between 20-25 micrometers in length and the cells themselves also lack a uniform shape, most are rounder, but the shape is determined by the formation of the cells around them (Cytion, 2024). Because of these properties, human keratinocytes are commonly used in studies to observe immunological and inflammatory responses. The majority of the epidermal layer is composed of keratinocytes and the skin has structural and barrier functions to the body. These attributes and the importance of epidermal health have made HaCaTs a popular model for studying inflammatory and immunological skin conditions, including burns (Colombo et al, 2017).

Fibroblasts are the most common type of connective-tissue cells in animals, they play an essential role in the formation of the extracellular matrix through the production of collagen, and because of this fibroblasts are essential for the structure and construction of tissue (Alberts B). This line of fibroblast cells, NIH-3T3, is one of the more popular cell lines, it originated in 1962 from mouse embryo fibroblasts In New York, the 3T3 part of the name is short for "3-day transfer, inoculum 3 x 10^5 cells"(Dastagir K). While fibroblasts are less differentiated than other connective tissue cells, fibroblasts from different organs of the body often behave as different subtypes of fibroblasts, in previous studies fibroblasts from the eyelid, back of the ear, and scar tissue behaved differently enough that the authors concluded they should be considered distinct cell types (Fernandes, I. R. et al). The fibroblasts taken pre-birth from the mouse embryos work well because they are composed of different fibroblast subtypes. Notably, fibroblasts also play a central role in wound repair for almost every part of the body through the production of a collagenous matrix. Because of this, and fibroblast's relatively easy culturing process, they have become popular for researching wound healing methods. Fibroblasts are also useful for producing induced pluripotent stem cells which, because they maintain all genetic background after the reprogramming, has caused fibroblasts to become a popular source for use in disease modeling in vitro (Fernandes, I. R).

Collagen is a structural protein found in skin and connective tissue. There are many types of collagen found in the body, exhibiting differences in the configuration of the protein molecules, the additional molecules attached to the collagen, and their respective locations within the body (Cleveland Clinic, 2022). Sigma 3D collagen is derived from bovine skin; it is sterile-filtered and concentrated at 2.9-3.2 mg/mL. An advantageous application of 3D collagen is its ability to form 3D matrices in cell culture. Collagen not only provides a scaffold for cells to structurally organize themselves around but also assists with cell adhesion (Lee et al., 2019). Replication of extracellular matrices in vivo, and in vitro allows for an accurate depiction of how cells associate with collagen (Sigma-Aldrich). Collagen being a biological component of the human organism promotes biocompatibility and reduces antigenicity when designing models that resemble the organismal environment of the cell (David, 2020). Given that experimental applications go beyond the lab, a biocompatible model ensures that results obtained from the experiment can be reflected in vivo.

Both rosehip and elderberry extracts are natural remedies that have indicated wound-healing properties, in particular, damage to epithelial cells (Valerón-Almazán et al, 2015). Initial research on both plants supports the historical use of rosehip and elderberry to treat wounds. Rosehip has been associated with the reduction of scar tissue through the prevention of inflammation and the promotion of macrophage activity. Rosehip efficacy is not only attributed to its antimicrobial and antioxidant properties, but also its chemical composition: fatty acids, polyphenols, vitamins B, C, and E, and carotenoids. According to Valerón-Almazán et al, groups treated with rosehip have shown significantly decreased rates of skin issues such as erythema, dyschromia, and atrophy. The healing capabilities of rosehip extract have been shown to promote healthier skin tissue healing compared to other scarred tissue (Belkhelladi et al, 2023). Additionally, elderberry also possesses antioxidant, anti-inflammatory, and antimicrobial properties, resulting in the promotion of wound healing through the induction of keratinocyte growth. In the research conducted by Weronika Skowrońska et al., they induced an inflammatory response in HaCaT and fibroblast cells that were grown in a monolayer and then treated with a 70% ethanolic elderberry extract and its fractions. A wound-healing assay revealed migratory HaCaT keratinocytes, supporting elderberries' wound-healing properties. Research showed increased cell migration and wound closure when treated with extracts and fractions compared to the medium (Skowrońska et al, 2024).

We intend to test and compare the effectiveness of elderberry and rosehip extracts by treating burned cells with each extract and comparing wound healing. In *Wound healing potential of extract from Sambucus nigra L. leaves and its fractions*, Skowrońska, and their team, tested the wound-healing properties of elderberry by growing a monolayer of HaCaT and fibroblast cells in 12 well plate cultures, scratching the cultured cells, treating the cells with the elderberry extract, and measuring cell proliferation in a migration assay (Skowrońska et al.). Our group plans to grow layers of HaCaT and fibroblast cells on a 3D collagen gel to simulate a burn wound on the colony of cells. The cells will be treated with rosehip and elderberry ethanol extracts, and utilizing a cell migration assay, we will analyze whether either extract promotes greater wound healing.

To quantitatively measure the effects of elderberry and rosehip extracts on burn healing, we will utilize tumor necrosis factor-alpha (TNF-α), a biomarker often elevated in burn victims. Burn injuries prompt an inflammatory reaction by the activation of multiple pathways, including mediators of the immune system cytokines. The reaction takes place immediately, with impairment in the function of neutrophils, an increase in T-suppressor cells, and a decrease in T-cells and natural killer cells. This kind of immune response is typically an indicator of organ failure and morbidity but it is dependent on the severity of the burn (Abdel-Hafez et al, 2007). TNF-α is an inflammatory cytokine produced by macrophages during inflammation and leads to signaling within cells causing necrosis or apoptosis (Idriss et al, 2000). This cytokine initiates the other responses to burn injuries by causing the release of interleukin-1 and interleukin-6, enhancing the response to burn injuries. In addition to initiating subsequent responses, TNF-α also increases vasodilation and capillary permeability (Sierawska et al, 2022). Studies have shown that TNF-α is increased in burn patients than in the control group, however, levels depend on the severity of the burn (Skowrońska et al, 2024). TNF-α is a proven biomarker that will allow us to study the effectiveness of these natural remedies.

METHODS AND PROCEDURES

General Cell Passaging

The NIH-3T3 (ATCC® CRL1658 ™) and HaCaT (AddexBio-T0020001) cell lines used for this procedure were passaged every 2 days over 6 weeks.. Complete medium, composed of Dulbecco's Modified Eagle Medium, 10% fetal bovine serum, and 1% penicillin/streptomycin (4°C), PBS (4°C), and trypsin (-20°C) was warmed in a 37 °C water bath. The cells were observed under a microscope to determine current confluency and then the passaging volume was determined. The hood and all cell passaging materials were sterilized with ethanol before the excess medium was aspirated out of the plate using a Pasteur pipette. 1 mL of PBS was added to the flask allowing 30 seconds to combine with cells and was then aspirated. 1 mL of trypsin was added to the flask, the flask was then placed back in the 37 C incubator for 10 minutes. Once the cells detached, depending on the volume of the flask, an amount of new medium was added to the flask. The previously determined amount of medium was removed from the old flask using a pipette and moved into a new labeled flask. Depending on the volume of the new flask, new medium was added to the flask which was then placed in a 37 C incubator until needed.

Preparation of Extract

Dried elderberry extract was purchased from Bulk Supplements, and dried rosehip extract was purchased from Alpi Nature. Stock 10% (w/v in ethanol) solutions of both extracts were prepared. 2.01 g of each supplement was dissolved in 20 ml of 70% ethanol. Each tube was vortexed for 1 minute to combine the powder and ethanol; both tubes were placed in a 65°C water bath for 1 hour for the powders to dissolve. The extracts were then filtered through a SteriFlip .22 µm filter and stored at -20°C until needed for treatment.

Collagen Preparation

6 mL of 2 mg/mL type I Collagen (Sigma-Aldrich-C4243), was prepared utilizing collagen solution from bovine skin. To prevent collagen from gelling, collagen was kept over ice. In a conical tube, 3.87 mL of 3.0 mg/mL of collagen was combined with 0.6 mL of PBS and 1.05 mL of DMEM. To neutralize the acidic pH of the collagen, 5µL of NaOH was incorporated into the collagen solution at a time until the solution was barely pink. 0.5mL of collagen was micropipette into each well of a 12-well plate. Before use, the collagen was permitted to solidify for 1-2 hours.

Wound Healing Assay

As a qualitative mode to determine healing, a wound healing assay was performed to depict the proliferation of the NIH-3T3 and HaCaT cells into the region of a burn wound inflicted on the cells. A 12-well plate was lined with 0.5mL of collage; a monolayer of HaCaT and NIH cells (1:1) were plated onto the collagen. The HaCaT and NIH cells were seeded into each well so that the final seeding density in a well was 5 x 10^5 cells. 1 mL of DMEM was added to each well. Cells were given 24 hours to adhere to the collagen before the assay was performed. To burn the cells, the media was aspirated from each well. An Aldrich® heavy-duty spatula was bent to the diameter of the well, to permit the square end of the spatula to lie flat over the layer of collagen. The Aldrich® spatula was sterilized and then heated 0.5 inches away from the flame of an alcohol lamp for 30 seconds. The spatula was briskly stamped vertically on the surface of the wells. Post-burn, 1mL of DMEM was added to each well. The cells were incubated for an hour at 37 °C; the delay in treatment mimics the time after injury in which a patient would receive care.

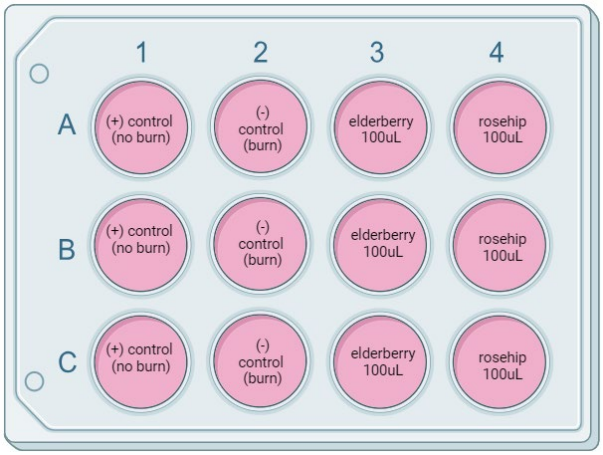

Figure 1. Model of 12-Well Plate

Cells receiving treatment were treated with 100µL of 10% elderberry or rosehip extract. In the experiment, the positive control was cells burned without any treatment. The negative control was cells burned and treated with 100µL of 70% ethanol (the solvent the extracts were made with). Treatment E was elderberry extract, while treatment R, was rosehip extract. After 24 hours, the media was

removed from the well; 1mL of new media was added into each well and the cells were treated with 100µL of extract or ethanol. 72 hours post burn, the treatment process was repeated. The proliferation assay was performed after two rounds (120 hours post burn).

Sample Collection

Samples were collected from the media, of each of the wells in the 12-well plate. Samples were collected before burn (0hr), 24, 72, and 120 hours post burn. From each well, 200µL of media was removed from the well and placed in a labeled 1 mL sterile tube. Samples were stored in a TEMP freezer for later use at -20 C.

Migration assay

The migration assay was performed after two rounds of treatment (120 hours post-burn) to visualize the proliferation of the cells. 0.5mL of 2% paraformaldehyde (PFA) was added into each well and allowed 30 minutes to process. The cells were washed once with 1X PBS. The cells were stained with three drops of 0.1% crystal violet (CV) for 20 min and put on a room temperature shaker at a low speed to ensure even stain distribution. The excess CV was aspirated and the cells were washed twice with 1X PBS. The plate was left uncovered to dry for 24 hours. The plate was observed under the microscope to visualize the proliferation of the cells into the burn wound.

Human TNF- a (Tumor Necrosis Factor Alpha) ELISA

Utilizing Elabscience® Human TNF- α (Tumor Necrosis Factor Alpha) ELISA Kit, a sandwich-Ab/Ag ELISA was conducted to determine levels of TNF-α secreted by the cells throughout the wound healing assay. Samples for ELISA were collected over different segments of time to understand the progression of TNF-α expression over a predetermined number of hours. 200 µl of sample was pipetted out of each well at zero hours post-treatment as well as 24, 72, and 120 hours. The samples were collected in individual labeled 1 mL microfuge tubes and separated by hour collected. Following collection the samples were stored in a -20 ℃ freezer until the ELISA was ready to be performed. According to the assay procedure, 100µL of diluted standard, blank and sample were added into the appropriate well as shown in Table 1.

Table 1. Model of ELISA Assay 48 Well Plate.

	1	2	3	4	5	6
A	24 hrs. (+) Control	72 hrs. (+) Control	120 hrs. (+) Control	24 hrs. (-) Control	72 hrs. (-) Control	120 hrs. (-) Control
B	24 hrs. (+) Control	72 hrs. (+) Control	120 hrs. (+) Control	24 hrs. (-) Control	72 hrs. (-) Control	120 hrs. (-) Control
C	24 hrs. (+) Control	72 hrs. (+) Control	120 hrs. (+) Control	24 hrs. (-) Control	72 hrs. (-) Control	120 hrs. (-) Control
D	24 hrs. Elderberry	72 hrs. Elderberry	120 hrs. Elderberry	24 hrs. Rosehip	72 hrs. Rosehip	120 hrs. Rosehip
E	24 hrs. Elderberry	72 hrs. Elderberry	120 hrs. Elderberry	24 hrs. Rosehip	72 hrs. Rosehip	120 hrs. Rosehip
F	24 hrs. Elderberry	72 hrs. Elderberry	120 hrs. Elderberry	24 hrs. Rosehip	72 hrs. Rosehip	120 hrs. Rosehip
G	blank	Standard 7.8	Standard 15.63	Standard 31.25	Standard 62.5	Standard 125
H	Standard 250	0 hrs. All Samples				

The plate was covered with sealer and incubated for 90 minutes at 37 ℃. The liquid from each well was decanted. immediately after incubation, 100µL of Biotinylated Detection Ab working solution was added to each well. The plate was covered with sealer and incubated for 1 hour at 37 ℃. The solution was decanted from each well, and 350µL of wash buffer was added to each well. The wash buffer was allowed 1 minute to soak and was aspirated from each well and pat dry against absorbent paper. This step was repeated 3 times. 100µL of HRP Conjugated working solution was added to each well. The plate was covered with sealer and incubated for 30 minutes at 37 ℃. The HRP Conjugated working solution was decanted from each well and the wash process was repeated 5 times. 90µL of Substrate Reagent was added to each well. The plate was covered with sealer and incubated for 15 minutes at 37 ℃. 50µL of Stop Solution was added to each well. The optical density of each well was determined using a microplate reader at 450nm.

RESULTS

MigrationAssay

To determine if elderberry or rosehip extracts increase the rate of proliferation post burn of a HaCaT and NIH-3T3 monolayer. TNF-α has been shown to increase in burn victims (include referenced). To determine the effect of rosehip and elderberry extracts on IL-6 secretion.

Table 2. Migration Assay

Field	1	2	3	4	5	Average	Triplicate Average
Control 1	3	2	2	4	0	2.2	7.67
Control 2	18	7	6	6	7	8.8	
Control 3	12	14	13	8	13	12	
Ethanol 1	1	5	1	0	1	1.6	2.33
Ethanol 2	2	4	0	4	2	2.4	
Ethanol 3	5	2	6	1	1	3	
Elderberry 1	N/A	N/A	N/A	N/A	N/A	N/A	9.4
Elderberry 2	N/A	N/A	N/A	N/A	N/A	N/A	
Elderberry 3	15	8	15	6	3	9.4	
Rosehip 1	27	10	17	9	30	18.6	22.6
Rosehip 2	22	28	35	23	25	26.6	
Rosehip 3	N/A	N/A	N/A	N/A	N/A	N/A	

In Table 2, five fields of view for each well were counted to determine the number of cells that had proliferated into the burn wound. The 12-well plate accommodates triplicates of the positive and negative controls, as well as the wells being burned and receiving treatment. The five fields of view of the well were averaged; the triplicate average was calculated by averaging the three wells of each control and each treatment.

Positive Control	Negative Control	Elderberry Well	Rosehip Well
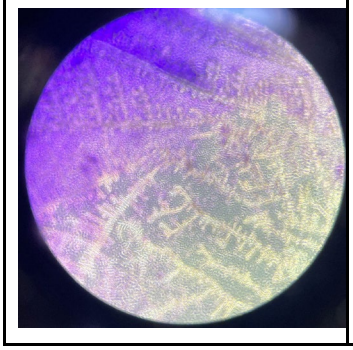	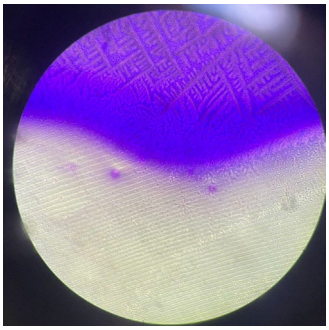	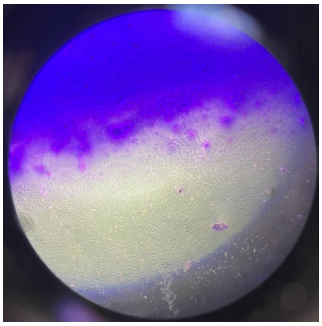	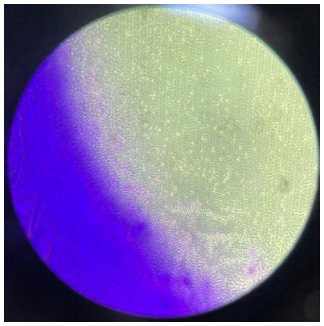

Figure 2. Migration Assay at 120 post-burn. Each image displays the edge of the burned section and the potential migration of cells into the burned area. Areas dyed with 0.1% crystal violet are live cells whereas undyed sections are where the burn occurred.

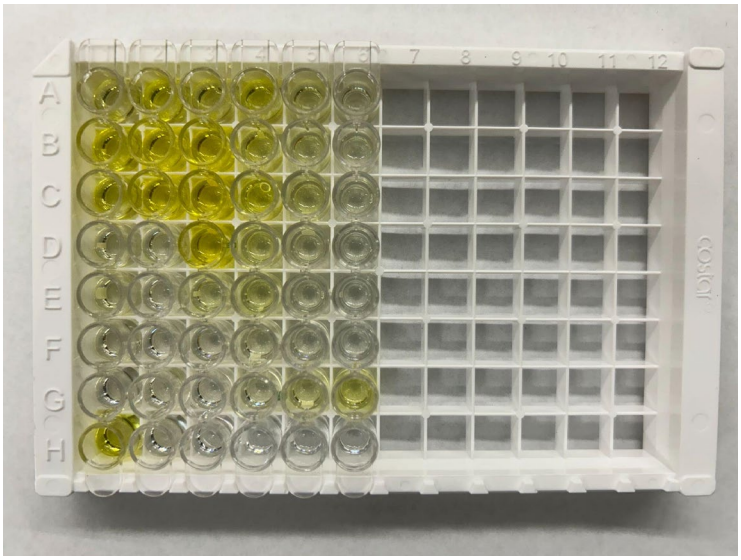

Figure 3. Completed ELISA Assay. This figure shows the assay after color development, color intensity is related to the optical density of TNF-α in each of the samples. Samples are loaded as depicted in Figure 1.

Table 3. TNF-α Optical Density Output

	1	2	3	4	5	6
A	0.218	0.412	0.274	0.385	0.178	0.108
B	0.812	1.23	1.164	0.25	0.152	0.092
C	0.353	1.094	1.279	0.369	0.164	0.088
D	0.115	0.09	1.222	0.177	0.083	0.068
E	0.126	0.091	0.147	0.173	0.083	0.063
F	0.091	0.062	0.073	0.09	0.066	0.051
G	0.062	0.094	0.069	0.103	0.156	0.245
H	0.447	0.047				

In Table 3 a microreader measured optimal density for each sample collected from the wound healing assay at 450 nm.

Table 4. TNF-α ELISA Standards Optical Density

Standards	Optical Density
7.8	*0.094*
15.63	0.069
31.25	0.103
62.5	0.156
125	0.245
500	0.447

In Table 4. the TNF-α ELISA Standards optimal density was measured by a microplate reader to create a standard curve.

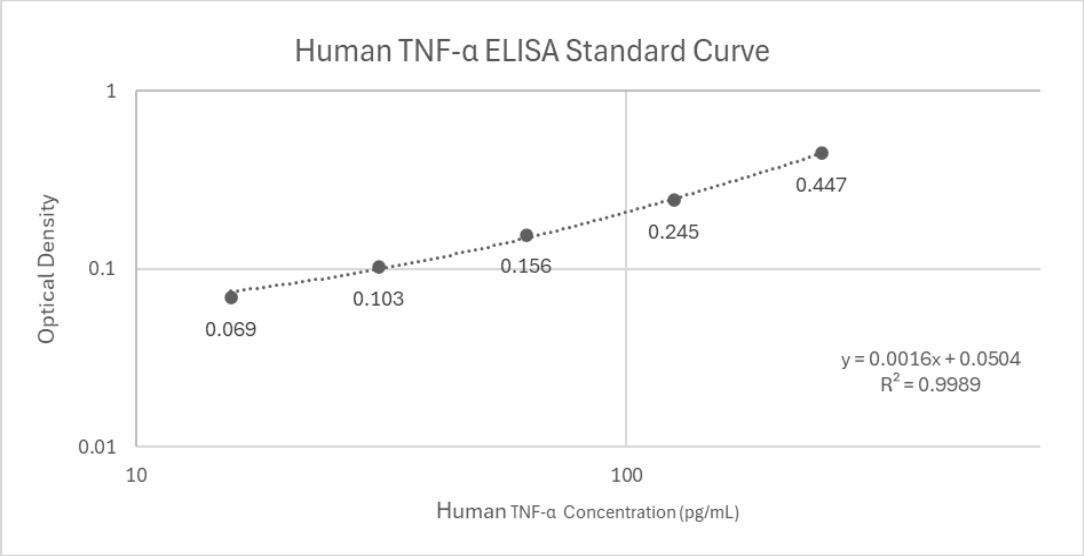

Figure 4. Human TNF-α ELISA Standard Curve. The standard curve of TNF-α was constructed by utilizing known concentrations of TNF-∝ and observing their optical density. The 7.8 (pg/mL) concentration was omitted for this for a more linear line of best fit.

Table 5. Concentrations from TNF-α ELISA

Averages	Positive (pg/mL)	Negative (pg/mL)	Elderberry (pg/mL)	Rosehip (pg/mL)
0 Hours	24.74	24.74	24.74	24.74
24 Hours	332.56	177.69	37.69	60.19
72 Hours	694.75	71.44	19.16	16.81
120 Hours	731.94	28.5	268.94	6.44

In Table 5 the concentrations of TNF-α was calculated for the samples collected from the wound healing assay that were determined utilizing the standard curve.

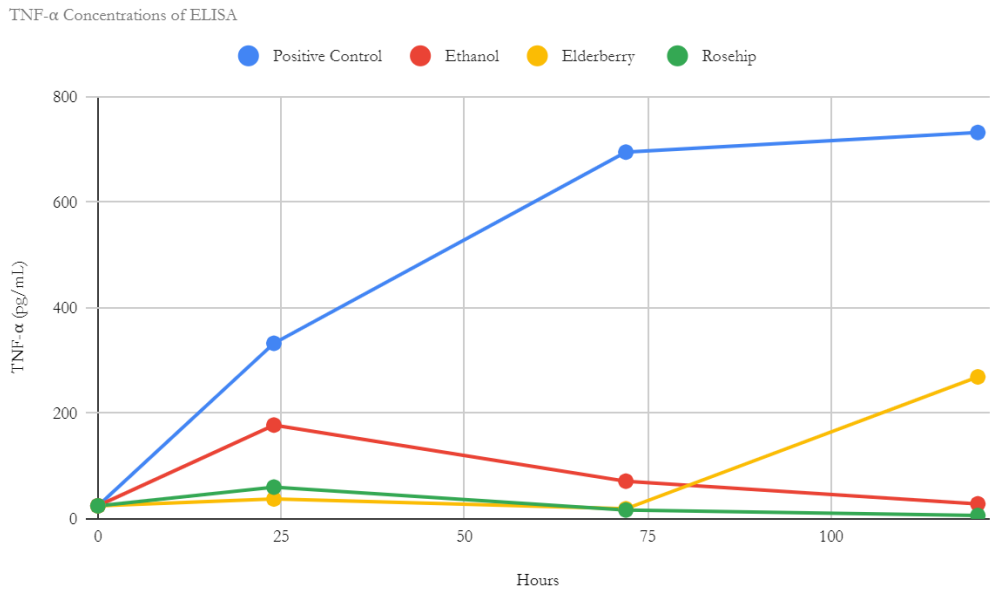

Figure 4. Optical Density of TNF-α Expression in Elderberry vs. Rosehip Treatments. The measured optical density of elderberry and rosehip treatments over the 120-hour treatment time.

DISCUSSION

To assess the healing effects of the natural remedies elderberry and rosehip on a burn wound, a migration assay was conducted to see the potential correlation between the movement of cells and the various treatments The cells were stained to determine migration into the burn wound only after 120 hours of burning the cells because staining at the times we collected samples from the media would have caused cessation of proliferation of the cells Following the staining process, the migration of cells was assessed after 120 hours by using five different fields of view within each burn of each well. The amount of cells that migrated into the burn was counted, averaged, and then compared to the other replicates within that treatment which can be seen in Table 2. Even though the intent was to burn each well evenly, after dyeing the wells it was obvious that the burns varied in depth causing difficulties in assessing migration. The wells for elderberry treatment 1 and 2 as well as rosehip treatment 3 were completely dyed and it was undecipherable where the burn was inflicted. Those wells experienced more surface-level burns whereas the rest of the wells experienced burns into the collagen layer. It is possible that those treatments experienced extreme migration but it is very unlikely when compared to the other wells of similar treatment. Due to this error, the migration of these wells could not be examined, making it difficult to say whether elderberry or rosehip was more effective at wound healing with the limited data available.

The results of the migration assay for the cells in both control groups are more conclusive as all three wells for both controls were countable. The average number of cells counted within the burned area in wells that were not treated was 7.67 and the average for wells treated with ethanol was 2.33. These results suggest that cells treated with ethanol had a significantly lower rate of migration into a burned area than cells that were not treated with anything. However, these results conflict with the concentrations of TNF-α found in Table 5 depicting concentrations of TNF-α from samples collected over the course of 120 hours post-burn. The predicted outcome of this assay was to show an increased level of TNF-α directly after the burn, then a steady decrease over time as the wound heals. The average levels of TNF-α in the non-treated wells greatly increased after the burn, as predicted, however, continued to increase over the course of the duration of the wound-healing assay. This would suggest that the wound is not healing effectively, as increasing levels of TNF-α indicates a need for a more extreme immune response from the body (Sierawska et al, 2022). Conversely, the wells treated with ethanol demonstrated the expected increase and decrease in TNF-α levels post burn, which would suggest successful wound healing. It is possible that the decreased levels of TNF-α in the ethanol treated wells is instead due to a lower number of surviving cells which could also cause a decrease in biomarker expression. This could be attributed to the fact that the final ethanol concentration in the wells of the cells treated with ethanol was 7%, which could have affected the cells ability to proliferate. Additionally, the decrease in TNF-α is also supported by the migration assay, given that the lack of surviving cells could also be attributing to a low migration of cells that received ethanol treatment

While the results of the migration assay for cells treated with rosehip extract are limited due to the failure of one of the three wells, the data that is present suggests that rosehip extract had the highest positive influence on migration rate out of all the treatments. There were 22.6 cells on average within the burned area in wells treated with rosehip, this is significantly greater then the average of 7.67 cells in positive control wells, and an average of 2.33 in the negative control indicating that rosehip extract promotes migration. This data is supported by the results of the ELISA assay seen in Table 5, which shows rosehip following the predicted rise and fall of TNF-α. The cells treated with rosehip showed a increase in TNF-α after being burned, then a steady decrease over the next two samples. Notably, the final TNF-α level of cells treated with rosehip is the lowest out of all treatment types. While the results are limited due to the failure of a well in the migration assay, the data from the migration assay and ELISA assay both support that

rosehip extract had the greatest positive influence on wound healing out of the treatments tested. However, it would be extremely beneficial moving forward to alter some of the methods and approaches to these experiments to achieve more conclusive results.

CONCLUSIONS

The migration assay reveals that the cells that did not receive treatment had a higher migration rate than the cells that were treated with ethanol. Ethanol was the solvent that was utilized to create the treatment extracts. Despite the 7% ethanol concentration in the wells, the cells triplicate average migration count was 2.33; indicating that the cells treated with ethanol were still able to migrate into the burn wound. Therefore, increased migration in cells that were treated with elderberry or rosehip treatments, utilizing ethanol as the solvent, point to the increased migration being attributed to the elderberry or rosehip extract. Given the inability of counting all of the wells treated with elderberry and rosehip, it is not clear whether or not elderberry or rosehip had an increase in migration; however, it appears that rosehip may have migrated more into the burn wound than cells treated with elderberry. The ELISA Assay revealed that cells that did not receive treatment continuously increased secretion of TNF-α , while cells that received ethanol treatment increased the secretion of TNF-α post-burn, and the levels decreased throughout the sample collection. Cells treated with elderberry treatment depicted conflicting increase and decrease of TNF-α levels throughout sample collection. Cells treated with rosehip treatment depicted an increase of TNF-α levels post-burn, and continuous decrease in TNF-α levels post burn.

In doing this experiment again, we would standardize the stamping of cells layered on collagen to ensure that the burns inflicted on the cells were consistent in all of the wells. Ensuring that the depth of the burn, and the ability to visualize in all the wells are consistent allows for comprehensive data collected from the migration assay. We intend to optimize the ethanol treatment by modifying the final concentration ethanol from 7% to 1% in the wells. At 1%, the ethanol level in the well would be more compatible with cell viability. Additionally, we would increase the replicate number, so that we have more data to conclude results from. We would take samples from the media post-burn every 24hrs, so that the fluctuation in TNF-α levels were captured more frequently throughout the healing process. Generally, it would be much more effective if the migration assay and the sample collection for the TNF-α were performed on different plates and if stained migration photos could have been taken at each of the predetermined hour marks while still being able to have biological replicates.

ACKNOWLEDGMENTS

The authors thank the Worcester Polytechnic Institute Biology and Biotechnology Department, Louis Roberts, Vanesa Lopa, and Shruti Shastry for their help in this research.

REFERENCES

1. 21 CFR 582.7724; U.S. National Archives and Records Administration's Electronic Code of Federal Regulations. Available from, as of June 21, 2006: https://www.ecfr.gov
2. Abdel-Hafez NM, Saleh Hassan Y, El-Metwally TH. A study on biomarkers, cytokines, and growth factors in children with burn injuries. Ann Burns Fire Disasters. 2007 Jun 30;20(2):89-100. PMID: 21991076; PMCID: PMC3188064.
3. Alberts B, Johnson A, Lewis J, et al. Molecular Biology of the Cell. 4th edition. New York: Garland Science; 2002. Fibroblasts and Their Transformations: The Connective-Tissue Cell Family. Available from: https://www.ncbi.nlm.nih.gov/books/NBK26889/
4. Belkhelladi M, Bougrine A. Rosehip extract and wound healing: A review. J Cosmet Dermatol. 2024; 23: 62-67. doi:10.1111/jocd.15971
5. Cleveland Clinic. "Collagen: What It Is, Types, Function & Benefits." Cleveland Clinic, 23 May 2022, my.clevelandclinic.org/health/articles/23089-collagen.
   "Collagen solution from bovine skin."
6. Collagen solution from bovine skin Sigma-Aldrich (sigmaaldrich.com)
7. Colombo I, Sangiovanni E, Maggio R, Mattozzi C, Zava S, Corbett Y, Fumagalli M, Carlino C, Corsetto PA, Scaccabarozzi D, Calvieri S, Gismondi A, Taramelli D, Dell'Agli M. HaCaT Cells as a Reliable In Vitro Differentiation Model to Dissect the Inflammatory/Repair Response of Human Keratinocytes. Mediators Inflamm. 2017;2017:7435621. doi: 10.1155/2017/7435621. Epub 2017 Dec 17. PMID: 29391667; PMCID: PMC5748104.
8. Dastagir K, Reimers K, Lazaridis A, Jahn S, Maurer V, Strauß S, Dastagir N, Radtke C, Kampmann A, Bucan V, Vogt PM. Murine embryonic fibroblast cell lines differentiate into three mesenchymal lineages to different extents: new models to investigate differentiation processes. Cell Reprogram. 2014 Aug;16(4):241-52. doi: 10.1089/cell.2014.0005. PMID: 25068630; PMCID: PMC4115680.
9. David, Geta. "Chapter 35 - Collagen-Based 3D Structures—Versatile, Efficient Materials for Biomedical Applications." ScienceDirect, edited by Kunal Pal et al., Elsevier, 1 Jan. 2020, pp. 881–906, www.sciencedirect.com/science/article/pii/B9780128168974000357. Accessed 26 Jan. 2024.
10. Fernandes, I. R., Russo, F. B., Pignatari, G. C., Evangelinellis, M. M., Tavolari, S., Muotri, A. R., & Beltrão-Braga, P. C. B. (2016, March). Fibroblast sources: Where can we get them?. Cytotechnology.

https://www.ncbi.nlm.nih.gov/pmc/articles/PMC4754245/#:~:text=Fibroblasts%20are%20cells%20widely%20used,easily%20accessible%20in%20the%20body.
11. HaCaT cells. CLS Cell Lines Service GmbH. (n.d.). https://www.cytion.com/HaCaT/300493
12. Hawley, G.G. The Condensed Chemical Dictionary. 9th ed. New York: Van Nostrand Reinhold Co., 1977., p. 788
13. Idriss HT, Naismith JH. TNF alpha and the TNF receptor superfamily: structure-function relationship(s). Microsc Res Tech. 2000 Aug 1;50(3):184-95. doi: 10.1002/1097-0029(20000801)50:3<184::AID-JEMT2>3.0.CO;2-H. PMID: 10891884.
14. Lee, A., et al. "3D Bioprinting of Collagen to Rebuild Components of the Human Heart." Science (New York, N.Y.), vol. 365, no. 6452, 2019, pp. 482–87, https://doi.org/10.1126/science.aav9051.
15. Pavez Lorie E, Stricker N, Plitta-Michalak B, Chen IP, Volkmer B, Greinert R, Jauch A, Boukamp P, Rapp A. Characterisation of the novel spontaneously immortalized and invasively growing human skin keratinocyte line HaSKpw. Sci Rep. 2020 Sep 16;10(1):15196. doi: 10.1038/s41598-020-71315-0. PMID: 32938951; PMCID: PMC7494900.
16. Sierawska O, Małkowska P, Taskin C, Hrynkiewicz R, Mertowska P, Grywalska E, Korzeniowski T, Torres K, Surowiecka A, Niedźwiedzka-Rystwej P, et al. Innate Immune System Response to Burn Damage—Focus on Cytokine Alteration. *International Journal of Molecular Sciences.* 2022; 23(2):716. https://doi.org/10.3390/ijms23020716
17. Valerón-Almazán, P. , Gómez-Duaso, A. , Santana-Molina, N. , García-Bello, M. and Carretero, G. (2015) Evolution of Post-Surgical Scars Treated with Pure Rosehip Seed Oil. Journal of Cosmetics, Dermatological Sciences and Applications, 5, 161-167. doi: 10.4236/jcdsa.2015.52019.
18. Weronika Skowrońska, Sebastian Granica, Jakub P. Piwowarski, Lejsa Jakupović, Marijana Zovko Končić, Agnieszka Bazylko, Wound healing potential of extract from Sambucus nigra L. leaves and its fractions,Journal of Ethnopharmacology, Volume 320, 2024, 117423, ISSN 0378-8741, https://doi.org/10.1016/j.jep.2023.117423. (https://www.sciencedirect.com/science/article/pii/S037887412301293X)

ABOUT STUDENT AUTHORS

Sarah Aspinwall will graduate in 2024 with a Bachelor's of Science in Biology and Biotechnology, Miles Williams will graduate in 2025 with a Bachelor's of Science in Biology and Biotechnology, and finally Sarah Oliveira will graduate in 2027 with a Bachelor's of Science in Biology and Biotechnology.

PRESS SUMMARY

Sambucus nigra L. commonly known as elderberry and the rosehip plants of the Rosa species are both prominent holistic remedies that have traditionally been used for their wound healing properties. This work intends to investigate the purported therapeutic properties of both plants when applied to a burn wound inflicted on a monolayer of cells grown over collagen gel. This was measured through a wound healing assay which counted the number of cells that migrated into the burn wound after treatment, and an ELISA assay which was used to measure the levels of tumor necrosis factor-alpha (TNF-α), a biomarker with increased levels in burn victims. These methods measured the severity of the burn and therefore the effectiveness of the treatments in promoting wound healing. The wound healing assay suggested that cells treated with elderberry extract demonstrated a similar level of migration to non-treated cells, while cells treated with rosehip extract had a greatly increased level of migration compared to cells that underwent any other treatment. The ELISA assay indicates that TNF-α levels decreased steadily post-burn in cells treated with rosehip, and decreased then sharply increased in cells treated with elderberry. This suggests that rosehip extract had a positive impact on burn healing as decreasing levels of TNF-α indicates decreasing burn severity. While this data is limited due to complications and time restraints it does indicate that rosehip extract possesses a level of healing properties and could potentially be used to therapeutic effect in the future.

Effects of Synthetic and Plant-Sourced Estrogen in Combination with Antioxidants on MCF-7 Cells

Grace Solod[a], Theresa Rosato[b], Samuel Levitan[a], Ren Vitellaro[a,c] & Louis Roberts[a]

[a]Department of Biology and Biotechnology, Worcester Polytechnic Institute, Worcester, MA
[b]Department of Biomedical Engineering, Worcester Polytechnic Institute, Worcester, MA
[c]Department of Chemistry and Biochemistry, Worcester Polytechnic Institute, Worcester, MA

doi.org

Students Emails: gcsolod@wpi.edu, trosato@wpi.edu, sblevitan@wpi.edu, lvitellaro@wpi.edu
Mentor Email: laroberts@wpi.edu

ABSTRACT
Breast cancer is one of the most prominent and deadly forms of the disease and the search for novel treatments is ongoing. The MCF-7 cell line is the most widely studied and well-understood human breast cancer cell line in the world. Previous research has shown MCF-7 cell's ability to metabolize estrogen, causing a downstream increase in reactive oxygen species (ROS). ROS have been found to cause an uptick in cell survival and proliferation. This project hypothesized that the treatment of MCF-7 cells with estrogen-like compounds would increase cell survival and division, whereas, treatment with an antioxidant would decrease MCF-7 survival and proliferation. MCF-7 cells were treated with different combinations of estrogen-like compounds (estradiol, biochanin, genistein, and whole soybean extract) and antioxidants (N-acetyl cysteine, curcumin, and ascorbic acid). A soft-agar assay, ROS-quantity assessment assay, and proliferation assay were conducted during and prior to cell treatment. While the ROS assay and soft-agar assay returned inconclusive, the proliferation assay showed decreased survival by cells treated with antioxidants. The cells treated only with an estrogen-like compound had vastly increased survival and proliferation. The results presented indicate the antioxidants tested reverse some increased survival and proliferation of MCF-7 cells caused by estrogen and phytoestrogens.

KEYWORDS
MCF-7 Cells; Breast Cancer; Estrogen; Estradiol; Phytoestrogens; Soy Beans; Antioxidants; Reactive Oxygen Species

INTRODUCTION

Cancer is a leading cause of death worldwide, with breast cancer killing over 685,000 people annually (WHO, 2023). As of 2020, 7.8 million women were living with breast cancer, 2.3 million of them having been diagnosed that year (WHO, 2023). This makes breast cancer the most prevalent cancer in the world (WHO, 2023). Early detection and treatment of breast cancer may improve one's prognosis. While treatments often involve surgery, radiation, or chemotherapy, the search for new therapeutic options is ongoing, as it has been found that attacking cancer from various angles via different treatment options is greatly beneficial (WHO, 2023). This study was done to investigate a novel approach to combating breast cancer through the use of antioxidant supplements, which are intended to act against estrogen-induced reactive oxygen species (ROS).

MCF-7s are human breast cancer cells derived in the 1970s from the pleural effusion of a metastatic breast cancer patient (*ScienceDirect Topics*, n.d.). These cells are highly useful in cancer research as they remain largely similar to the cancerous mammary epithelium (*ScienceDirect Topics*, n.d.). As such, MCF-7s process estrogen as estradiol through the use of highly upregulated estrogen receptors within the cells (*ScienceDirect Topics*, n.d.). The importance of this capability, in studying the estrogen receptor and beyond, is difficult to overstate as MCF-7s are the most abundantly studied breast cancer cell line (Lee et al., 2015). In addition to being estrogen receptor (ER) - positive, MCF-7 cells are progesterone receptor (PR) - positive (Comşa et al., 2015). As such, the cells are a member of the luminal A molecular subtype, making MCF-7 cells a part of the cell subtype that represents a majority of all breast cancers; thus calling to the importance of studying such cells (Yersal & Barutc, 2014).

Necessary for their proliferation, MCF-7 cells rely on estrogen (E2) for survival (Comşa et al., 2015). ER expression often fluctuates in the cells, with its expression increasing when the cells are in the absence of estrogens (Comşa et al., 2015). Other crucial receptors harbored by MCF-7 cells for their survival and proliferation include HER2 and the EGFR (Comşa et al., 2015). In terms of this

research, MCF-7 cells have proved crucial in that they interact with and metabolize estrogen. Through these metabolic reactions, reactive oxygen species (ROS) are produced. Appropriate physiological concentrations of ROS are important to cell survival, but their overproduction is characteristic of several disease types, including cancer. In fact, it is known that cancer cells are typically exposed to higher ROS levels, which in turn stimulate malignant behaviors such as death evasion, angiogenesis, invasiveness, and metastasis (Hecht, 2016). This is due to the fact that cancer cells exhibit heightened metabolic and proliferation rates that can only be supported by increased ROS levels (Sosa, 2013). With this in mind, there are broader implications of ROS regulation in cancer treatment, and many chemotherapeutic drugs already employ ROS modulation to influence tumor outcome.

Roy et. al. investigated the role of estrogen-induced reactive oxygen species (ROS) in breast cancer. MCF-7 breast cancer cells, as well as T47D breast cancer cells, were treated with natural estrogen, 17 beta-estradiol (E2), and synthetic estrogen, diethylstilbestrol (DES). Separately, some cells received an antioxidant in addition to either the E2 or the DES. The ROS that resulted from the subsequent estrogen metabolism were analyzed with a DCF-DA (dichlorofluorescin diacetate) assay, and cell proliferation was quantified with an MTT (3-(4, 5-dimethylthiazol-2)-2, 5-diphenyltetrazolium bromide) assay. It was discovered that both the natural and the synthetic estrogen increased the amount of ROS. Both estrogens also induced growth in both breast cancer cell types. Further cell cycle analysis using flow cytometry confirmed that the ROS were the reason for this increased growth in the MCF-7 cells. Protein expression analysis through Western blots revealed that the ROS caused epigenetic reprogramming in the present cells. The inclusion of antioxidant treatment seemed to restore the function of regulatory proteins that were negatively impacted by epigenetic reprogramming. This discovery holds potential for therapeutic applications with continued research and testing. Moreover, Roy et. al. confirmed that estrogen-induced ROS are responsible for increased growth in breast cancer cells. This study demonstrates the importance of cell lines that can be utilized for scientific research, including the cell type that we are working with, MCF-7. The current study presented hoped to further investigate antioxidant treatment for reducing estrogen-induced growth, including an exploration of antioxidant supplementation to slow or limit cell proliferation and growth.

METHODS AND PROCEDURES

Growing and maintaining MCF-7 cells

MCF-7 Cells (ATCC, Catalog No. HTB-22) were obtained and cultured at 37 °C at 5% CO_2. Cells were passaged in complete media containing 1% penicillin-streptomycin, 10% fetal bovine serum (FBS), and Dulbecco's Modified Eagle Medium (DMEM) (Corning, Catalog No.10-013-CV), and detached from flasks using 5% trypsin. Cells were routinely passaged every two days before they were seeded in assays.

Creating extracts

Over-the-counter antioxidant supplements were used to create extracts for N-acetyl cysteine (NAC) (NAC 1,000 mg per 2 capsules with Selenium & Molybdenum, Spring Valley), curcumin (Turmeric Curcumin with Ginger Powder 500 mg per capsule, Spring Valley), and ascorbic acid (Chewable C 500 mg, Nature Made). The NAC and curcumin supplements were in capsule forms. For each antioxidant, one capsule was broken and the powder was used to create extracts in 80% methanol. 2mM NAC and 10uM curcumin extracts were created. The ascorbic acid supplement was in chewable form. One tablet was pulverized with a mortar and pestle and the resulting powder was used to create a 2mM extract in 80% methanol. The extracts were kept in a water bath at 37°C for approximately 72 hours until the solute was completely dissolved. The resulting extracts were used in each of the following assays.

Two estrogen extracts in 80% methanol were created using pre-existing stock samples as follows: 10 nM estradiol was created from $5x10^{-3}$ M β-estradiol (E8875-250MG) and 6 uM biochanin was created from $2.6x10^{-3}$ M biochanin. A 5 uM genistein extract in 80% methanol was created using pure genistein powder (EMD Millipore Corp., Catalog No. 345834-20MG). The extract was kept in a water bath at 37°C for approximately 72 hours until the solute was completely dissolved. Full soybean extract was taken from a pre-existing project's stock. The resulting extracts were used in each of the following assays.

Soft-agar assay

To assess cells ability to colonize in an anchorage-independent environment, a soft agar assay was completed using agarose. Sterilized 1% agar was combined with an equal volume of medium containing charcoal-stripped serum and 1.5 mL was plated at the bottom of each well in each 6-well plate. Plates were cooled in the fridge until use 48 hours later. Sterilized 0.6% agar was combined with an equal volume of medium containing charcoal-stripped serum and 1.5 mL was combined with 250 uL of each treatment. This solution was pipetted on top of the bottom layer and allowed to set at room temperature. Plates were moved to 37 °C at 5% CO_2 and incubated for 7 days. 2 times a week, 100 uL of medium using charcoal-stripped serum was pipetted on top of each well. Plates were stained using c stain and images were taken using (**explain microscope here**).

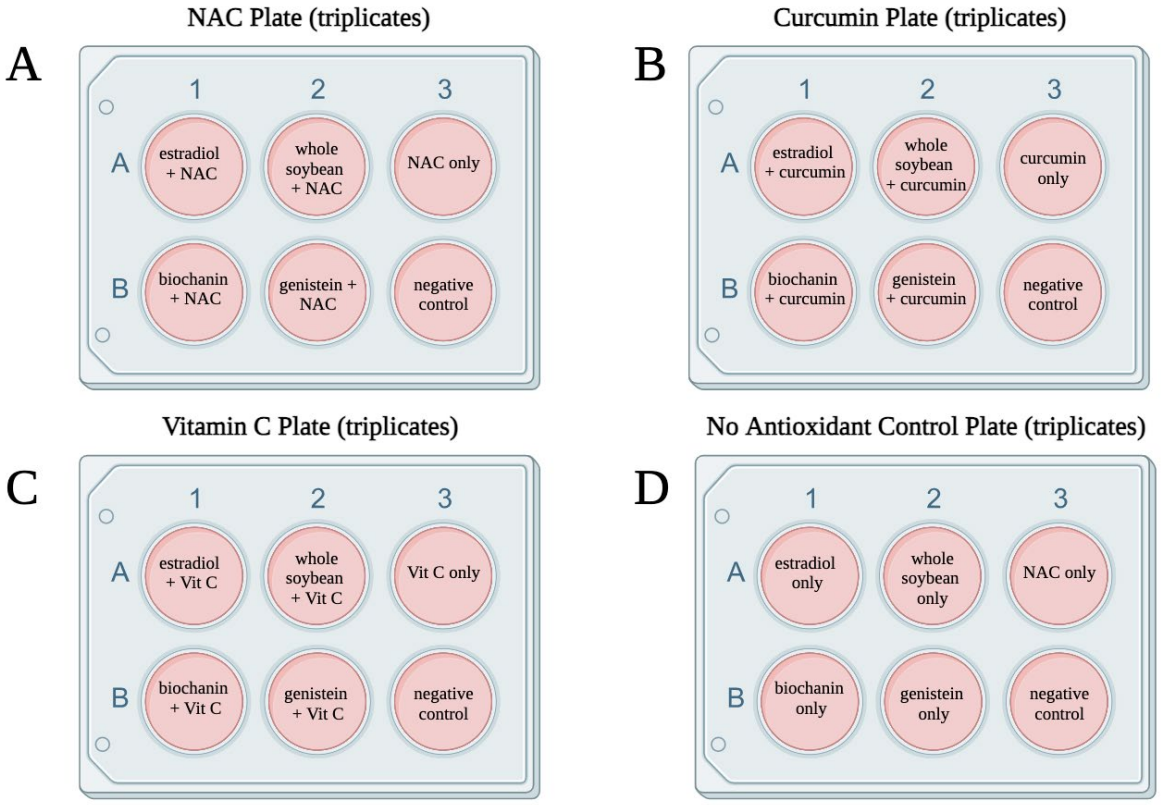

Figure 1. Plate Layouts for Soft Agar Assay. One plate was used for each antioxidant condition, with a different estrogen-like compound in each well. One well on each plate was a negative control and contained no antioxidant or estrogen. Panel A tests NAC, Panel B tests curcumin, Panel C tests Vitamin C, and Panel D tests no antioxidant.

Alamar Blue Resazurin proliferation assay

To assess cellular activity after treatment with estrogen and antioxidants, a proliferation assay was completed using the Alamar Blue Cell Viability Reagent (Invitrogen, Catalog No. DAL1025). Cells were seeded at a density of $1*10^5$ in column 2 then 1:2 dilutions were made through column 8. To create blanks, column 9 had no cells and was filled with media and treatments. Plates were incubated at 37 °C at 5% CO_2 for 48 hours. One well without treatment was trypsinized and counted using the Cellometer Auto T4 Plus Cell Counter (Nexcelom Bioscience LLC, Serial No. AutoT4-301-9232). Wells were treated with the Alamar Blue reagent then each plate was read for fluorescence (in RFUs) using a 540 nm excitation wavelength and a 590 nm emission wavelength. The RFUs of blank wells were subtracted from treated wells so that the resulting RFU value is representative of cells only. The RFUs were converted to cell counts based on the control well that was counted before Alamar Blue staining.

ROS assessment assay

To assess the quantity of cell-produced ROS after treatment with estrogen and antioxidants, a DCFH-DA assay was completed using the HaDCFDA Reagent (Sigma Aldrich, Catalog No. D 6883). 100µL of cells at 1 x 10^5 cells/mL was used to seed the necessary wells of a 96-well plate. Cells were incubated at 37 °C at 5% CO_2 in charcoal-stripped media with their respective estrogen-like compound and/or antioxidant condition at 10% each, including positive and negative controls, for 48 hours. Each condition of estrogen-like compound/antioxidant -- or lack thereof -- was done in triplicate. After the incubation period, the media was aspirated, the cells were washed with 100µL of 1X PBS and then stained with 100µL of 10,000x diluted HaDCFDA in a 1:1 mix of 1X PBS and charcoal-stripped media. The cells were incubated in the dark at 37 °C at 5% CO_2 for 72 hours. After the 72-hour incubation period, liquid in the wells was aspirated and 100µL of 1X PBS was added. The plate was red for RFUs using a 540 nm excitation wavelength and a 590 nm emission wavelength. The RFUs of blank wells were subtracted from treated wells.

RESULTS

Soft-agar assay

To assess the proliferation and colonization capabilities of the MCF-7 cells under varying treatment conditions, a soft-agar assay was performed. *Figure 2* below shows an example of the images captured with the microscope. *Table 1* below shows the results of this assay, which was the average number of colonies formed by MCF-7 cells in one frame of reference under the microscope. A generally observed trend was that, for the curcumin and vitamin C plates, the no-treatment wells had greater colonization than the estrogen-treatment

wells. This indicates that treatment with either of these antioxidants could correlate to decreased metastatic activity. The NAC plate, on the other hand, saw greater colonization with the estrogen-treated wells than the no-treatment wells, indicating that treatment with NAC might not be an effective way to limit metastatic activity. There were some exceptions to these trends within the data, but this could likely be due to a low number of replicates per condition.

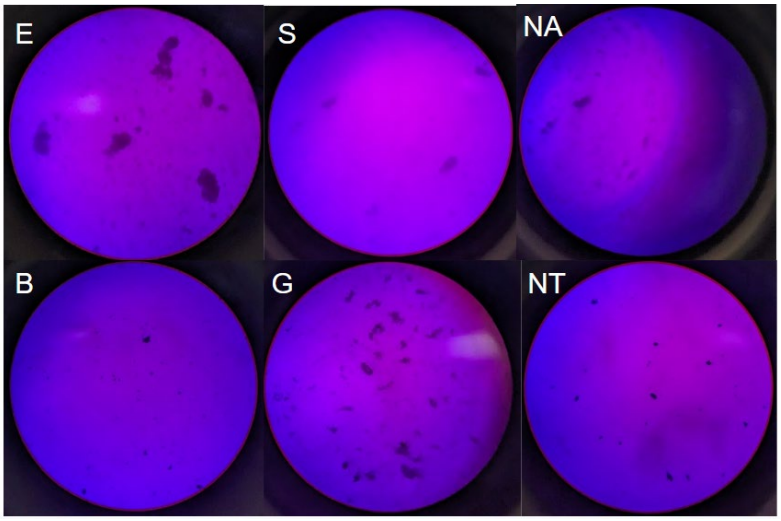

Figure 1. This figure shows an example of the images taken for data collection on the soft-agar assay. The image was taken at 100x magnification and shows 6 frames of the estrogen only plate. E indicates estradiol, S indicates soybean extract, NA indicates no antioxidant, B indicates biochanin, G indicates genistein, and NT indicates No Treatment.

Table 1. Average Results from Soft Agar Assay

	Estradiol	**Soybean**	**Antioxidant only**	**Biochanin**	**Genistein**	**No treatment**
NAC	2.5	7	4	6	3.5	3
Vitamin C	4	4	1	1.5	0	16
Curcumin	7	2.5	6.5	0.5	2	4
No Antioxidant	4.5	4	15*	9.5	6	4*

Table 1 shows the average results from the soft agar assay. Images were taken from one frame of reference in each well of the 6 well plate, for two replicates of each condition. The colonies present in each of the images were counted and the average of the two replicates was recorded in the table above.
* For the no-antioxidant plate, the "antioxidant only" well contained neither estrogen nor antioxidant extracts, therefore was the same as the no-treatment condition.

Proliferation assay

In the Rezasurin survival assay, cells were treated with estradiol and various antioxidants, and a standard curve was developed, as shown in *Figure 2*. Cells with no treatment had the highest survivability (slope of 1661.7 RFU/cell count, Table 2) based on the slope of the linear fit. Cells treated with only estradiol had the next highest survivability at (slope of 1768.6 RFU/cell count, Table 2). Finally, all three antioxidants significantly dropped the cell's survivability, but the differences in slope between the three antioxidant conditions were not significant based on standard deviations. Vitamin C had the least effect on the cells treated with estradiol (Figure 2).

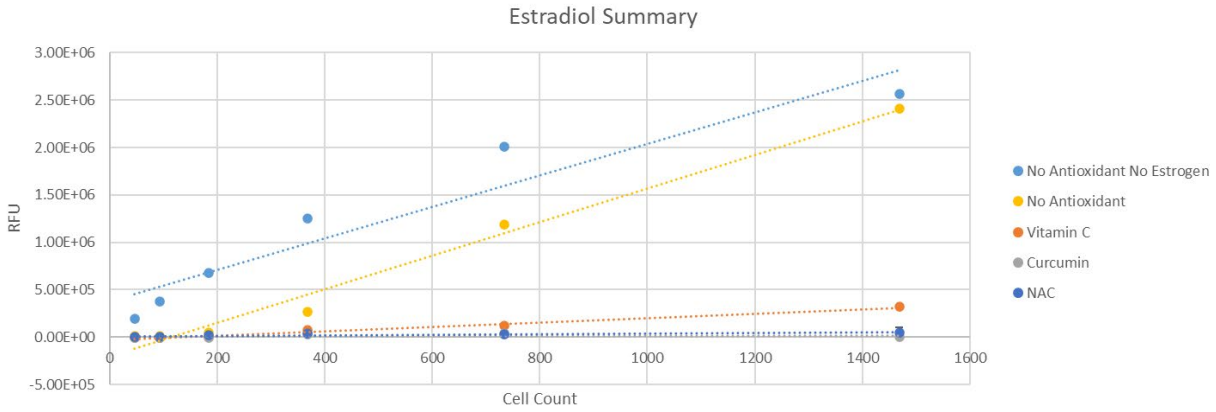

Figure 2. Resazurin assay dilution series for each condition with estradiol compared to control without antioxidants. Dotted lines are linear regressions for each condition. Error bars are one standard deviation. X axis is cell count and Y axis is RFU reading normalized to wells with matching treatments and media with no cells.

Table 2. Survivability Slope for Estradiol Samples

Estradiol:

Sample	**Slope**
No A no E	1661.7
No A	1768.6
Vit C	230.8
NAC	31.3
Curc	6.8

Table 2 shows the average survivability (slope of linear fit) for each estradiol condition shown in Figure 2. A higher slope indicates higher cell survival in the media conditions.

Figure 3 shows results from the resazurin survival assay, where cells were treated with biochanin and three antioxidants. Based on the series of dilutions, a standard curve was developed. Cells with no treatment had the highest survivability based on the slope of the linear fit. Cells treated with only biochanin had the next highest survivability at (1346.8 RFU/cell count, Table 3). Finally, all three antioxidants significantly dropped the cell's survivability, but the differences in slope between the three antioxidant conditions was not significant based on standard deviations (Figure 3).

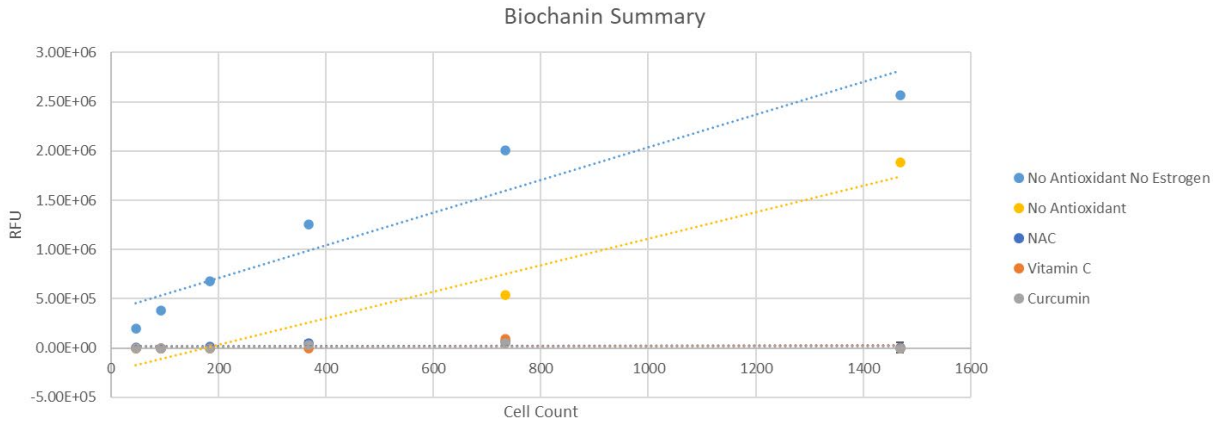

Figure 3. Resazurin assay dilution series for each condition with Biochanin compared to control without antioxidants. Dotted lines are linear regressions for each condition. Error bars are one standard deviation. X axis is cell count and Y axis is RFU reading normalized to wells with matching treatments and media with no cells.

Table 3. Survivability Slope for Biochanin Samples

Biochanin

Sample	**Slope**
No A no E	1661.7
No A	1346.8
Vit C	13.6
NAC	6.6
Curc	6.14

Table 3 shows the average survivability (slope of linear fit) for each biochanin condition shown in Figure 3. A higher slope indicates higher cell survival in the media conditions.

Figure 4 shows results from the resazurin survival assay, in which cells were treated with the phytoestrogen genistein and three antioxidants. Based on the series of dilutions, a standard curve was developed. Cells with no treatment had the highest survivability based on slope of the linear fit. Cells treated with only genistein had the next highest survivability at (1509.9 RFU/cell count, Table 4). Finally, all three antioxidants significantly dropped the cell's survivability, but the differences in slope between the three antioxidant conditions was not significant based on standard deviations (Figure 4).

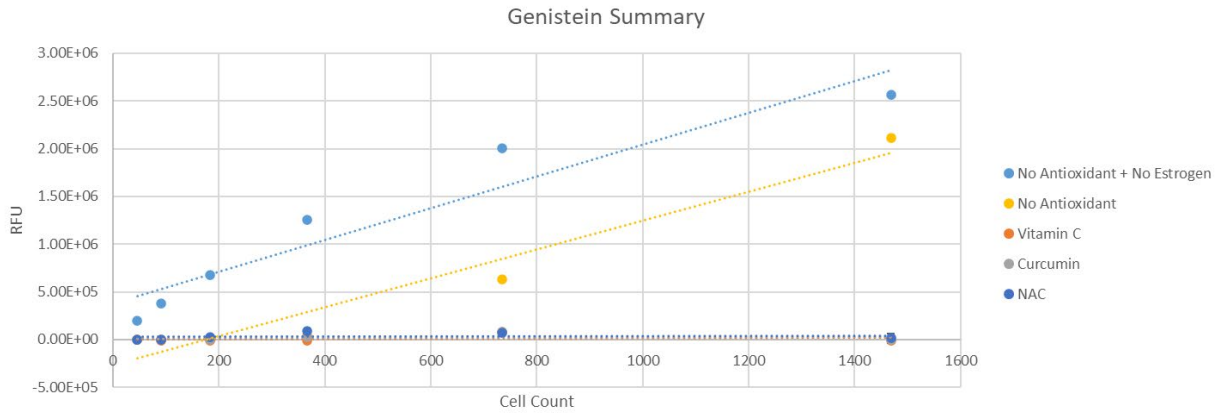

Figure 4. Resazurin assay dilution series for each condition with genistein compared to control without antioxidants. Dotted lines are linear regressions for each condition. Error bars are one standard deviation. X axis is cell count and Y axis is RFU reading normalized to wells with matching treatments and media with no cells.

Table 4. Survivability Slope for Genistein Samples

Genistein

Sample	**Slope**
No A no E	1661.7
No A	1509.9
Vit C	13.3
NAC	10.9
Curc	11.8

Table 4 shows the average survivability (slope of linear fit) for each genistein condition shown in Figure 3. A higher slope indicates higher cell survival in the media conditions.

Figure 5 shows the resazurin survival assay, in which cells were treated with whole soybean extract in methanol and three antioxidants. Based on the series of dilutions, a standard curve was developed. Cells with no treatment had the highest survivability based on slope of the linear fit. Cells treated with only soybean had the next highest survivability at (1748.4 RFU/cell count, Table 5). Finally, all three antioxidants significantly dropped the cell's survivability, but the differences in slope between the three antioxidant conditions was not significant based on standard deviations (Figure 5).

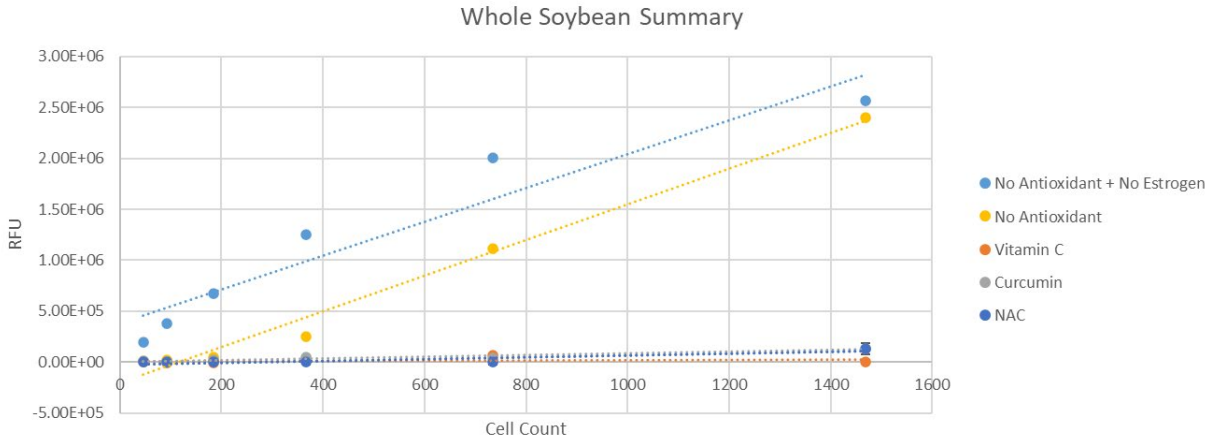

Figure 5. Resazurin assay dilution series for each condition with whole soybean extract compared to control without antioxidants. Dotted lines are linear regressions for each condition. Error bars are one standard deviation. X axis is cell count and Y axis is RFU reading normalized to wells with matching treatments and media with no cells.

Table 5. Survivability Slope for Whole Soybean Extract Samples

Whole Soybean

Sample	**Slope**
No A no E	1661.7
No A	1748.4
Vit C	11.5
NAC	87.2
Curc	82.4

Table 5 shows the average survivability (slope of linear fit) for each whole soybean condition shown in Figure 3. A higher slope indicates higher cell survival in the media conditions.

Table 6. 1:4 Dilution Summary of Cell Proliferation in RFU

1:4 Dilution	*No Estrogen*	*Estradiol*	*Biochanin*	*Genistein*	*Whole Soybean*
No Antioxidant	*1958537*	*1184392*	*535910*	*631254*	*1119161*
NAC		*31500*	*69351*	*75925*	*189*
Vitamin C		*117723*	*95262*	*78828*	*66855*
Curcumin		*36659*	*44990*	*79261*	*37334*

Table 6 shows the average RFU reading for the 1:4 dilution for each condition. The no antioxidant condition consistently had the most cell growth while the three conditions containing antioxidants significantly impaired cell proliferation. The condition with neither estrogen nor antioxidant had the overall highest proliferation.

ROS assay

Upon measurement of plate fluorescence, no clear pattern or general difference between control and experimental groups was visualized. Furthermore, the values were highly disparate between the same trials done in triplicate. Variability with the data can be attributed to the use of a low-concentrated stain, and due to the time constraints of the project, the assay was not able to be repeated. For these reasons, the data collected from the ROS assay was disregarded in further analysis.

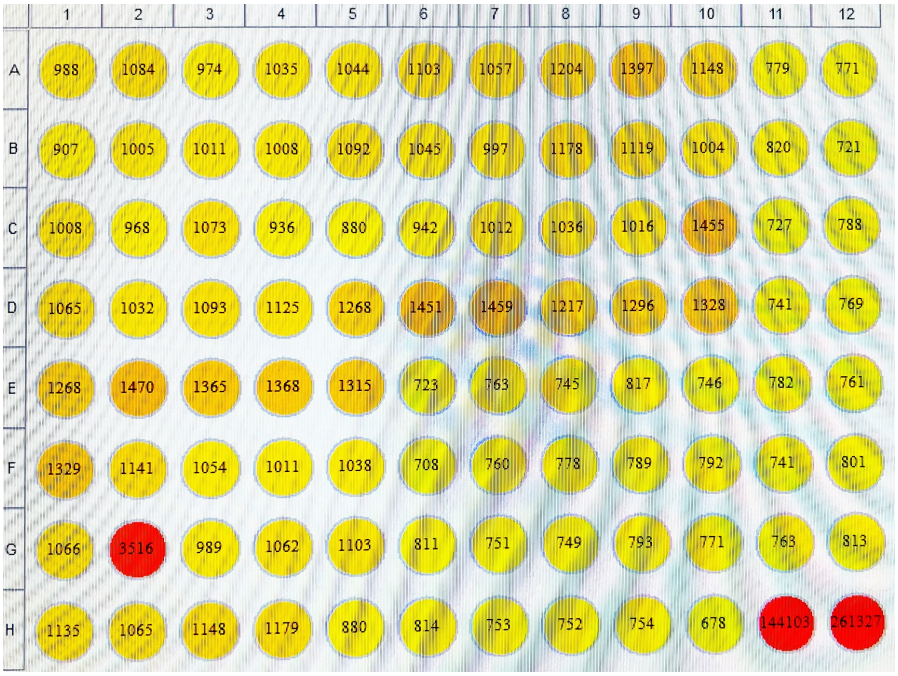

Figure 6. Fluorescent readout from ROS assay showing no clear difference between estrogen and antioxidant treatment combinations. The bottommost wells on the right side with notably higher RFUs are blanks containing the HaDCFDA reagent.

DISCUSSION

The data presented above shows that there is evidence of antioxidants decreasing the growth, proliferation, and survival of MCF-7 cells. As seen broadly from the proliferation assay data, cells in the absence of antioxidants had the highest survival and division. This effect increased when those same cells were treated with an estrogen-like compound. Consistently, the highest RFU values, indicating high survival and proliferation, were from cells without antioxidants and cells treated with an estrogen-like compound and no antioxidant. Cells treated with no antioxidants or estrogen like compound had a higher survivability than those treated with estrogen (Table 6). This

was opposite to what was expected since estrogens increase the proliferation rate of cancer cells. One explanation for this could be cytotoxicity of the methanol and water that the extracts were made in. A good control for future experiments could be cells grown in base media plus methanol and water to see how growth is affected. Cells treated with antioxidants, even when exposed to estrogen-like compounds, had the lowest RFU values and, thus the lowest survival and proliferation. According to the proliferation assay linear regression, the antioxidant curcumin frequently resulted in the lowest projected proliferation. On the other hand, vitamin C was often an outlier in its effect on the proliferation assay. This may be due to it having different interactions with the various estrogen-like compounds used or the concentration was less harmful to the cells.

Referencing the soft-agar assay, the aforementioned trend in data is most evident in cells treated with biochanin and genistein where the "no antioxidant" group had over three colonies more than the next highest well. Regarding cells treated with antioxidants, NAC-treated cells seemed to have the highest growth whereas vitamin C-treated cells had some of the lowest. More research needs to be done into appropriate treatment concentrations and including negative controls for the media and treatment solvents.

Unfortunately, there was no discernible pattern from the ROS assay data. It is believed that the dye was too far diluted and unable to make a strong enough signal.

Overall, there is a clear trend in cells treated with antioxidants having lower survival and proliferation while estrogen-like compound treated cells had increased growth and division. These data support the use of antioxidants as a tool to decrease MCF-7 cell proliferation and colony formation.

CONCLUSIONS

This study is an early, broad approach to investigating the effects of estrogen-like compounds and antioxidants on the survival, growth, and proliferation of MCF-7 breast cancer cells. The data presented indicates a correlation between treatment with various antioxidants and decreased MCF-7 proliferation; and, conversely, treatment with estrogen-like compounds with increased MCF-7 proliferation. These findings align with previous studies that implicate high ROS levels in increased cancer cell proliferation and malignant behavior. Metabolism of the estrogen-like compounds is thought to result in heightened ROS levels, though we were unable to confirm this specifically. However, based on the findings from our proliferation assay, it is clear that the estrogen-like compounds play a role in increasing MCF-7 proliferation, despite not being able to identify the mechanism through which this occurs. The role of ROS is somewhat illuminated by the demonstrated decrease in MCF-7 proliferation when treated with antioxidants, which reduce oxidative stress and autoxidation. Concentration assays would be beneficial to understand what concentrations of antioxidants are most effective at slowing growth of cells without being cytotoxic. As noted, the current study is an early investigation with a broad swath of estrogen-like compounds and antioxidants. More research is needed into specific compounds and their mechanism of action to fully understand the changes in cell growth and proliferation witnessed.

ACKNOWLEDGMENTS

The authors thank Professor Lou Roberts, TAs Shruti Shastry and Vanesa Lopa, and peers in their class.

REFERENCES

Comşa, Ş., Cîmpean, A. M., & Raica, M. (2015). The Story of MCF-7 Breast Cancer Cell Line: 40 years of Experience in Research. *Anticancer Research*, *35*(6), 3147–3154.

Hecht, F., Pessoa, C. F., Gentile, L. B., Rosenthal, D., Carvalho, D. P., & Fortunato, R. S. (2016). The role of oxidative stress on breast cancer development and therapy. Tumor Biology, 37(4), 4281–4291. https://doi.org/10.1007/s13277-016-4873-9

Lee, A. V., Oesterreich, S., & Davidson, N. E. (2015). MCF-7 Cells—Changing the Course of Breast Cancer Research and Care for 45 Years. *JNCI: Journal of the National Cancer Institute*, *107*(7), djv073. https://doi.org/10.1093/jnci/djv073

Roy, P., Kandel, R., Sawant, N., & Singh, K. P. (2024). Estrogen-induced reactive oxygen species, through epigenetic reprogramming, causes increased growth in breast cancer cells. Molecular and Cellular Endocrinology, 579, 112092. https://doi.org/10.1016/j.mce.2023.112092

Sosa, V., Moliné, T., Somoza, R., Paciucci, R., Kondoh, H., & LLeonart, M. E. (2013). Oxidative stress and cancer: An overview. Ageing Research Reviews, 12(1), 376–390. https://doi.org/10.1016/j.arr.2012.10.004

World Health Organization. (2023, July 12). Breast cancer. https://www.who.int/news-room/fact-sheets/detail/breast-cancer

Yersal, O., & Barutca, S. (2014). Biological subtypes of breast cancer: Prognostic and therapeutic implications. *World Journal of Clinical Oncology*, *5*(3), 412–424. https://doi.org/10.5306/wjco.v5.i3.412

Topical Antioxidants in the Recovery of UV Exposed Collagen Skin Models

*Jamie Baines[a], Hayden Bovard[b], William Miller[b], & Louis Roberts[*b]*

[a]Department of Biomedical Engineering, Worcester Polytechnic Institute, Worcester, MA
[b]Department of Biology & Biotechnology, Worcester Polytechnic Institute, Worcester, MA

Students: jlbaines@wpi.edu, hsbovard@wpi.edu, wamiller@wpi.edu
*Mentor: laroberts@wpi.edu**

ABSTRACT
Skin cancer is one of the most common types of cancer in the United States. Exposure to ultraviolet radiation has been shown to be a major risk factor in the development of skin cancer. Keratinocytes and fibroblasts are responsible for making up the top layers of skin, the epidermis and dermis. Skin models made from 3D collagen were created to understand the effects of antioxidant treatments on ROS levels present in the skin after exposure to UV light. Vitamin E, vitamin C, and vitamin B3 are all antioxidants that neutralize ROS through the addition of hydrogen atoms or inhibiting ROS generation entirely. The collagen skin models with embedded NIH 3T3 cells and top layer of HaCaT cells were exposed to UV light for a set duration. Antioxidant treatments of vitamin E, vitamin C, and vitamin B3 were applied to models following UV exposure. After initial exposure and two days following, the proliferation and ROS levels of the models were measured and analyzed. This study supports the theories that vitamins E and B3 are effective at reducing ROS levels in seeded collagen models, ROS reduce cell viability, UV irradiation of a collagen skin model using HaCaTs and NIH3T3 cells increases initial ROS levels, and UV radiation intensity seems to fall off as it passes through seeded collagen, but cannot definitively be used to conclude the effects of vitamins on the healing process after UV irradiation.

KEYWORDS
3D collagen; fibroblasts; keratinocytes; UV irradiation; antioxidants; reactive oxygen species; hydrogel; Vitamin E; Vitamin C; Vitamin B3; resazurin

INTRODUCTION
Melanoma is a very common type of cancer, colloquially referred to as skin cancer. One in five of Americans are expected to develop melanoma by the age of 70, making it a significant public health issue [1]. The overwhelming majority of melanoma cases are due to excessive exposure to sunlight, specifically the ultraviolet (UV) light present in sunlight. Prevention measures obviously include applying sunscreen, avoiding prolonged exposure, and wearing clothes with a sun protection factor (SPF) value, but treatment methods can vary. Common treatments include topical creams such as aloe vera and hydrocortisone, with the goal of these treatments being to alleviate pain and reduce inflammation. These treatments are palliative in nature, meaning that they do not cure or treat the underlying cause of the ailment. Vitamins C, E, and B3, to name a few, are known for their antioxidative properties, which could make them an effective treatment for sunburn. Reactive oxygen species (ROS) are at the core of the damage that characterizes sunburn, and antioxidants are very effective at neutralizing those species, so, theoretically, these vitamins could be used as a non-palliative treatment for sunburn.

Ultraviolet (UV) light from the sun is known to cause damage to the skin when there is either a lack of protection for the skin, or prolonged exposure to sunlight, or both. This happens due to the creation of reactive oxygen species, which are oxygen-containing free radicals, meaning that they react readily and rapidly with other molecules within and around cells in the skin. These reactions destabilize and destroy critical parts of the cell, such as the cell membrane and DNA. The nucleic acids that make up strands of DNA can be directly affected by these ROS, causing guanine to be modified, which allows it to bind to both cytosine and adenine [2]. Such modifications can lead to improper base pairing and therefore genetic mutations or breaks in the DNA, which can cause cancer or cell death. Proteins and lipids can also be affected, causing amino acid side chains to oxidize, and therefore change shape, preventing them from functioning as intended [2]. Lipids in the cell membrane undergo peroxidation when exposed to UV, which can both damage the membrane and create harmful products which affect other aspects of the cell. UV light also reduces the effectiveness of the enzyme catalase, which is used to neutralize hydrogen peroxide, a potent ROS, leading to the buildup of more and more ROS over time [3].

Niacin and vitamins E and C are all antioxidants, meaning that they help to neutralize ROS, the harmful class of molecules produced by UV light exposure. Vitamins E and C donate a hydrogen atom to ROS to neutralize them, preventing things like lipid peroxidation

from taking place and damaging cells [4]. Vitamin C helps to regenerate vitamin E so that it can continue providing its antioxidative benefits [4]. Niacin inhibits ROS generation, as well as prevents the oxidation of low-density lipoproteins, which are a major component of atherosclerosis [5]. Vitamins E and C, as well as niacin, are commonly consumed as supplements, and vitamin E is also used as a topical oil to treat scarring, sunburn, and overall skin health.

HaCaT is an immortalized cell line of keratinocytes, non-tumorigenic and monoclonal in nature [6]. Derived from the skin tissue of a 62-year-old man, and thus *Homo sapiens*, the cells are utilized in the study of epidermal characteristics such as growth and response to various conditions as they display the same morphology, surface markers, and functions of keratinocytes [6]. The cells form an adherent monolayer with a doubling time of roughly 28 hours, though can also be cultured in a 3D structure of compatible biomaterial such as collagen. Interestingly, these cells can form stratified layers in the presence of Ca2+ and differentiate back and forth depending on its concentration; low Ca2+ maintains a basal state while high Ca2+ differentiates to a more granular state [6]. As touched upon previously, HaCaT cells can be utilized to study the characteristics and responses of keratinocytes; the most common models of assessment on these cells are those of inflammatory responses and repair mechanisms, aiding in the understanding and potential development of therapeutics related to skin disorders and/or their proceeding diseases [6].

NIH 3T3 is an immortalized cell line of fibroblasts derived from a mouse embryo in 1962 [7]. The cells are utilized in the study of fibroblastic characteristics such as mechanistic behaviors and response to various conditions, though they are extremely heterogeneous, fibroblasts are mesenchymal cells integral to connective tissue and forming the framework of various tissues [7, 8]. The NIH 3T3 cell line is adherent with a doubling time of between 20-26 hours, they can form a monolayer or also be cultured in a 3D structure of compatible biomaterial such as collagen. Notably, due to the heterogeneous nature of the line, it is highly recommended that homogeneous sub-cell lines of the NIH3T3 line be created for more advanced research as the presence of various differentiated cell lines will alter results [8]. The potential research of the NIH3T3 cell line is vast as they serve as a foundation for better understanding tissue connectivity, scaffolding, wound healing, and various diseases such as fibrosis [8].

To recreate a simplified skin model for this experiment, two cell types were seeded within and on a 3D collagen model. To represent the epidermal layer of skin, the keratinocytes that are consistently produced within its layers are modeled using the HaCaT cells described previously in a monolayer seeded above the 3D collagen model [9]. Within this collagen model, to represent the dermis that consists of low cell density fibroblasts in a dense collagen matrix, the previously described NIH 3T3 cells are seeded in its formation [9]. While human skin consists of many more layers, with various cell types, than represented by our model, such as the dendritic cells and melanocytes found within the stratum spinosum and stratum basale respectively, we believe that the two aforementioned cell types to be implemented in a collagen matrix provide a sufficient medium for this UV based experiment [9].

Collagen is a common natural biomaterial that is used in cell culture models. It is a major structural protein of bone, tendon, skin, and cornea in humans and other animals. For use in modeling, collagen molecules extracted from bovine skin are dissolved in an aqueous solution and sterile filtered to make type I collagen solution [10]. When brought from a colder temperature to room temperature, collagen solution sets to a gel, giving this material the ability to be mixed with water-based solutions to form hydrogels [11]. The solution gels when the protein forms fibrils that self-assemble into bundled fibers that form a matrix structure. Factors such as collagen concentration, temperature, and pH can all affect the density and gelation rate of 3D collagen [11]. Due to its gel structure, 3D collagen is a great material to use for *in vitro* models. Because collagen gels are at a physiological temperature, cells can be embedded into 3D collagen to make hydrogels and scaffolds. These properties are why collagen is commonly used in tissue engineering, wound healing, and mechanobiology applications to make 3D matrices as it provides similar physiological conditions for cells [10]

METHODS AND PROCEDURES

Cell Culture and Preparation

NIH-3T3 (ATCC, Catalog No. CRL-1658) and HaCaT (AddexBio, Catalog No. T0020001) cells were cultured at 37°C and 5% CO_2 in Dulbecco's Modified Eagle Medium (Gibco, DMEM(1X)) with additives of 1x penicillin-streptomycin and 10% fetal bovine serum (FBS) (Corning). Cells were passaged with 0.25% trypsin-EDTA every 2-3 days prior to use in experiment.

3D Collagen Skin Model

To make the 3D skin model, NIH-3T3 cells were embedded in 3D collagen gel with a monolayer of HaCaT cells seeded on the top. As the model's purpose is to represent skin, the cell embedded collagen was plated 2 mm thick to mimic the dermis, which ranges in thickness from 1 to 4 mm [12]. To create the models, 0.7 mL of 3D collagen gel embedded with NIH-3T3 fibroblasts was plated in 2 12-well plates (CellTreat) to make a total of 18 models.

The final gel solution had a composition of 88% 3D collagen solution to 22% cell suspension. To make the collagen gel solution, 9.03 mL of 3.1 mg/mL Type I rat tail 3D collagen (Sigma-Aldrich, Catalog No. C4243) 1.2 mL 10X PBS, 1.2 mL of complete media, and 50 µL of 1M NaOH were combined in a 50 mL conical tube. The cell suspension was created from a confluent T-75 flask of NIH-3T3 cells with approximately 1.33 x 10^5 cells/mL. The flask was trypsinized with 2 mL of 0.25% trypsin, counted, and centrifuged for 5 minutes at 3000 rpm. The pellet was resuspended in 3.15 mL of complete media to achieve a cell concentration of 5.06 x 10^5 cells/mL. The final gel solution was made from 11.43 mL of the 3D collagen gel solution and 2.57 mL of fibroblast cell suspension to make 14 mL of gel with a 2 mg/mL collagen density and 1 x 10^5 cells/mL cell density. To add the cell embedded collagen to the well

plates, 700 µL was added and the plates were placed in the incubator at 37°C and 5% CO_2 for approximately 24 hours to set. After 24 hours had passed, HaCaTs were seeded on top of the collagen gels. Confluent HaCaT cells, approximately 7.17 x 10^5 cells/mL, were trypsinized from a T75 flask with 0.25% trypsin. The cell suspension was counted and then diluted with complete media to achieve a concentration of 1.82 x 10^5 cells/mL. To each model, 1 mL of HaCaT cell suspension was added, resulting in approximately 1.82 x 10^5 cells to be seeded on top of each gel.

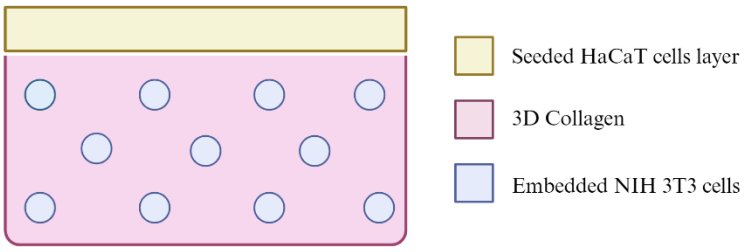

Figure 1. 3D Collagen Skin Model (Created with BioRender.com).

UV Irradiation Application

A UV lamp (Crystal, BioGlow®, Model No. BG-42-AA) was used to apply UV irradiation with a wavelength of 365 nm to the skin models. The lamp was placed directly on top of the well plate and switched on for 10 minutes. Wells that did not need UV exposure were covered by a piece of aluminum foil.

	1	2	3	4
A	10 mins UV expos. + Day 2 ROS assay		No UV expos. + Day 2 ROS assay	No UV expos. + Day 0 ROS assay
B	10 mins UV expos. + Day 2 Resazurin assay	10 mins UV expos. + Day 0 Resazurin assay	No UV expos. + Day 2 Resazurin assay	No UV expos. + Day 0 Resazurin assay
C	10 mins UV expos. + Day 0 ROS assay			

Table 1. UV Exposure Plate Set up on a 12-well plate.

Antioxidant Treatment Preparation and Application

To prepare the antioxidant treatments, forms of vitamin E, vitamin C, and niacin or vitamin B_3, were mixed in complete media. To make the vitamin E serum, 1 vitamin E gel capsule (Spring Valley, 180 mg) was added to 6 mL of complete media and the solution was placed in the water bath to dissolve. The oil from the capsule did not fully dissolve in the medium, so the serum was mixed thoroughly before 1 mL was added to the desired wells. To make the vitamin C serum, 0.3g of ascorbic acid was added to 3 mL of complete media. The solution was thoroughly mixed to ensure the powder was fully dissolved before 1 mL was added to the desired wells. To make the niacin/vitamin B_3 treatment, 1 capsule (Spring Valley, 500 mg) was emptied into a conical tube with 5 mL of complete media. An additional 10 mL of complete media was added to the treatment solution to dissolve the powder. After thoroughly mixing, 1 mL of the supernatant from the serum was added to the desired wells.

	1	2	3	4
A	10 mins UV expos. + Vitamin E + Day 2 ROS assay	10 mins UV expos. + Vitamin C + Day 2 ROS assay	10 mins UV expos. + Niacin/Vitamin B3+ Day 2 ROS assay	
B	10 mins UV expos. + Vitamin E + Day 2 Resazurin assay	10 mins UV expos. + Vitamin C + Day 2 Resazurin assay	10 mins UV expos. + Niacin/Vitamin B3+ Day 2 Resazurin assay	
C				

Table 2. Vitamin Treatments Plate Set up on a 12-well plate.

Microscopy

The photos taken, and seen below, were taken using the standard camera on an iPhone 11. The photos were taken from the lens of a light microscope at 100x magnification and were simply stabilized for optimal imaging using hands against the lens.

Resazurin Assay

The resazurin assays of this experiment were conducted to determine the cell counts/proliferation of the various tested parameters/controls from initial UV exposure to two days after exposure. Resazurin was applied to the collagen skin models with cells in 1mL of media. As each well contained total 1.7mL volume of both media and the collagen model, the resazurin was added to each at 170uL to achieve a 10% dilution. Once added, the wells were allowed to incubate at 37C and 5% CO2 for 24h before recording the results using (absorbance/fluorescence) at (nm) in a (plate reader?). The results of the experimental wells were referenced against control resazurin wells and the control models.

Cellular ROS Assay

To measure the level of ROS present in the models at different points during their treatment, the DCFDA / H2DCFDA - Cellular ROS Assay Kit (product code ab113851) from Abcam was used. Media was aspirated from the collagen models, and 1mL of 1x PBS buffer was used to rinse the gels. The buffer was then aspirated as well, after which 1.09mL of the 20μM DCFDA reagent was added. Plates were then incubated for two days. Post incubation, the reagent was aspirated and 1mL of 1x PBS buffer was added. With the PBS still in the well, the fluorescence of the wells was measured using a PerkinElmer VICTOR^3 Multilabel Plate Reader. An untreated collagen model was used as a blank.

RESULTS

Skin Model Images

	Top Layer	Bottom Layer
Control	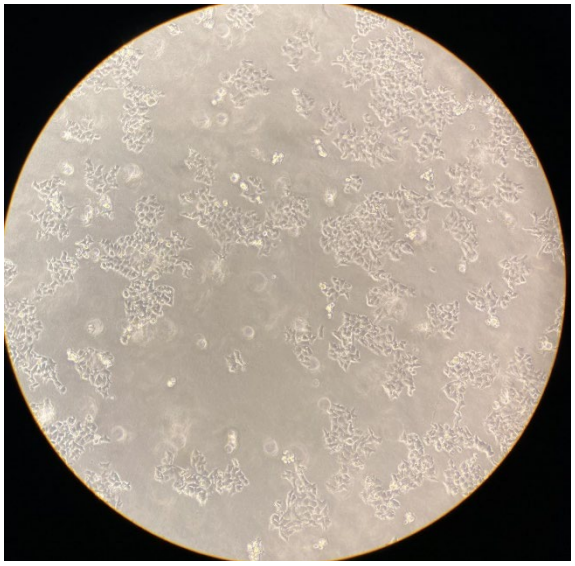	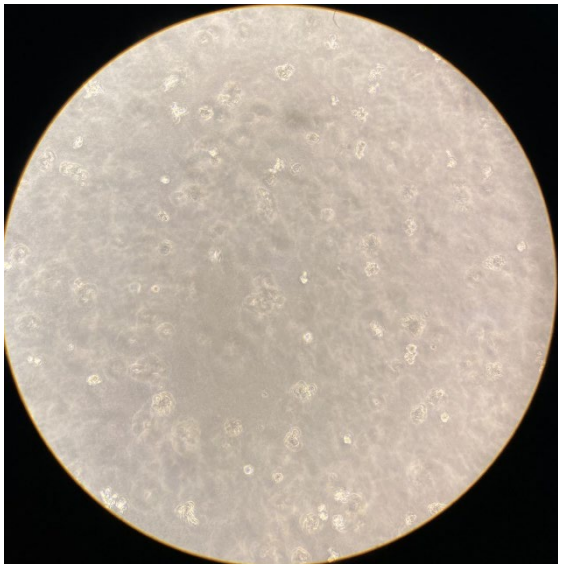
5 Minutes UV	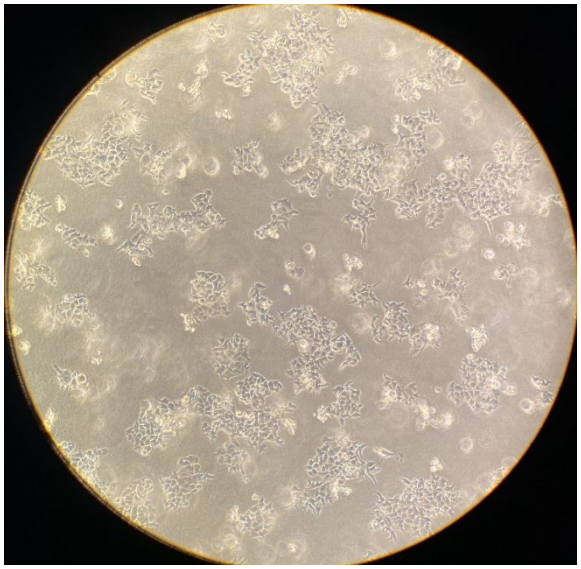	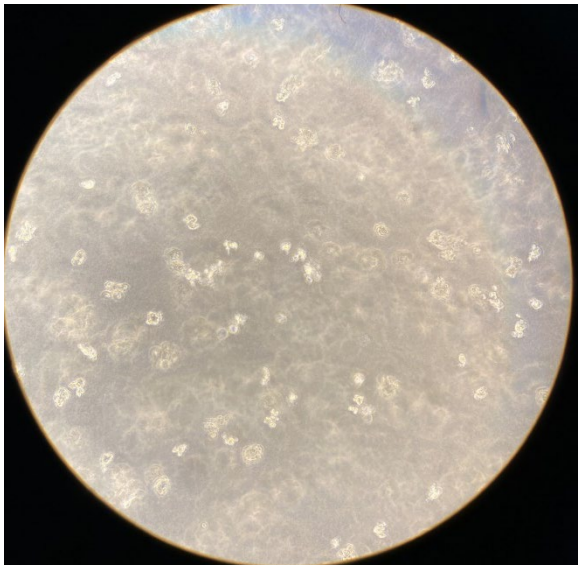
15 Minutes UV	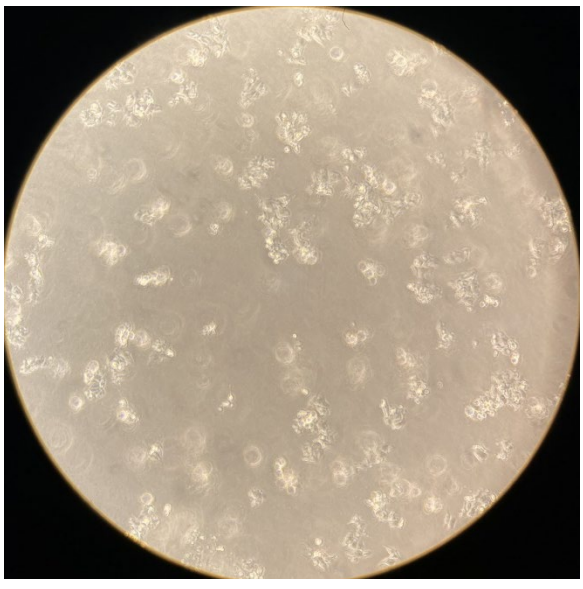	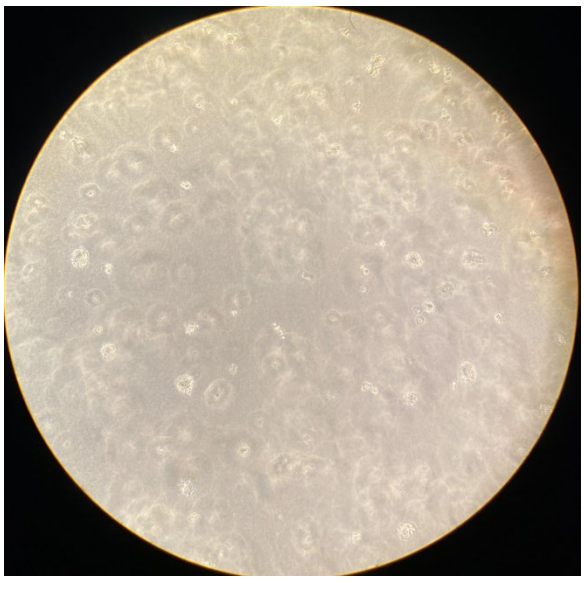

30 Minutes UV

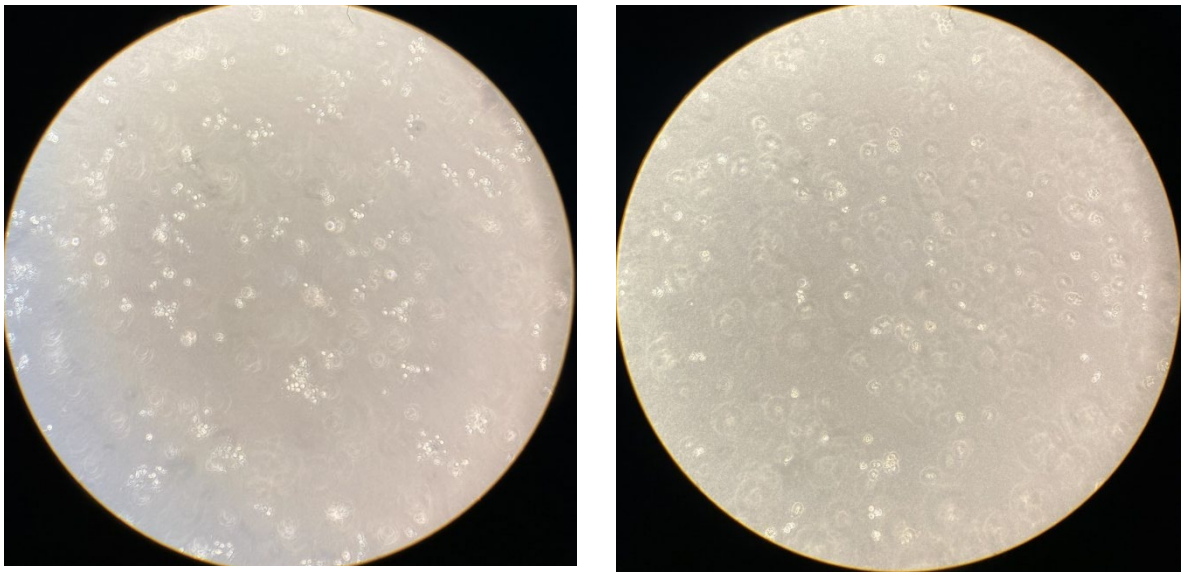

Figure 2. Images of NIH3T3 seeded 3D collagen gels after the three varying UV, 365nm, exposure times: 0 minutes control, 5 minutes, 15 minutes, and 30 minutes after 2 days. Imaging both the lower and upper most sections of the collagen model at 100x.

Top Layer **Bottom Layer**

Control Skin Models

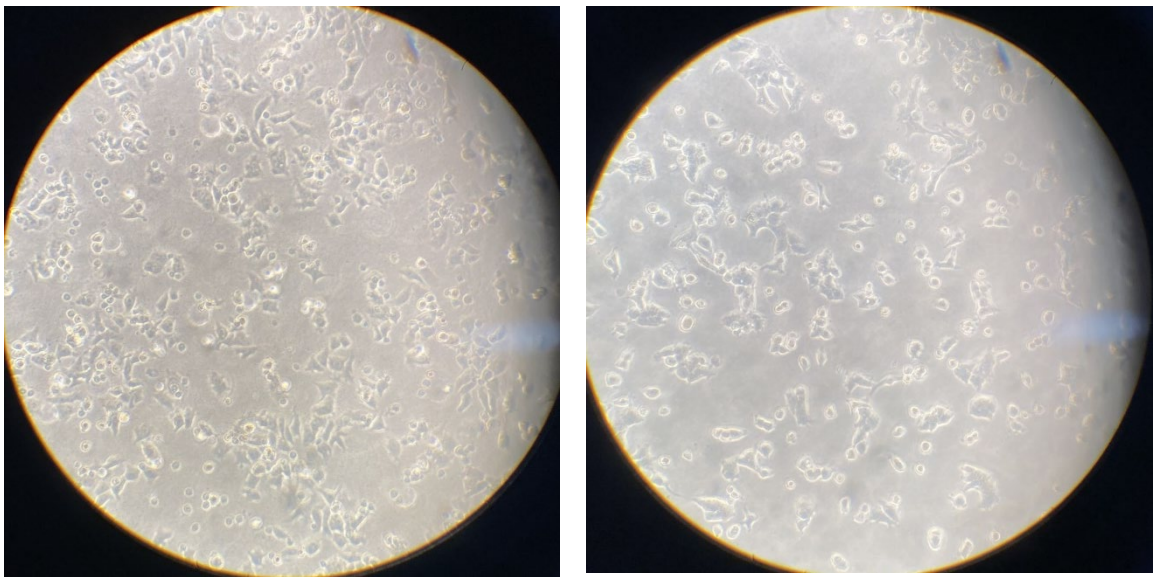

Figure 3. Images of NIH3T3 seeded 3D collagen gels and seeded HaCaT top monolayer before 10-minute UV exposure. Imaging both the lower and upper most sections of the collagen model at 100x.

Figures 2 and 3 display the most superficial and most basal layers of the collagen models with cells present. The non-UV exposed models of both figures display more cell confluency on their most superficial layer relative to their most basal layer. While, in figure 2, the 5-minute UV exposed model retains this quality, the models exposed to UV for 15 and 30 minutes display a decreased confluency of cells at their most superficial layer relative to the most basal layer that appears to remain consistent across all the models.

	Top Layer Old Media	Bottom Layer Old Media	Top Layer New/No Media	Bottom Layer New/No Media
Negative Control No UV	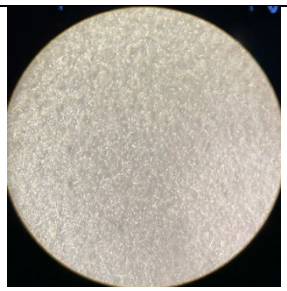	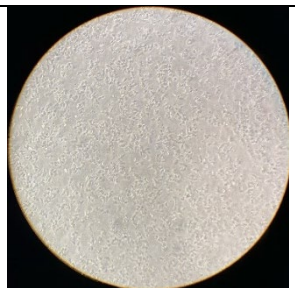		
Positive Control 10-minute UV Exposure	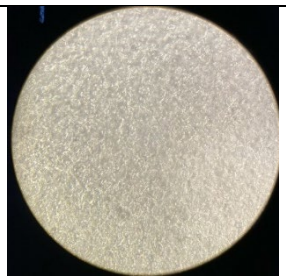	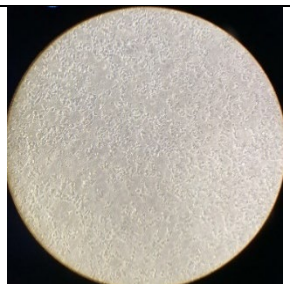		
Vitamin E 10-minute UV Exposure	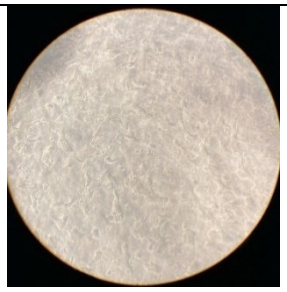	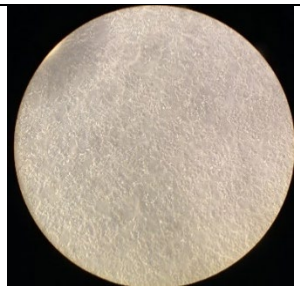		
Vitamin C 10-minute UV Exposure		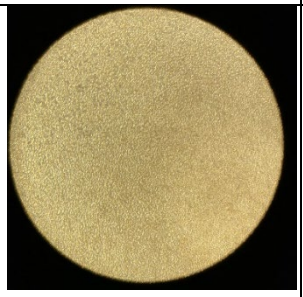		
Vitamin B, 10-minute UV Exposure	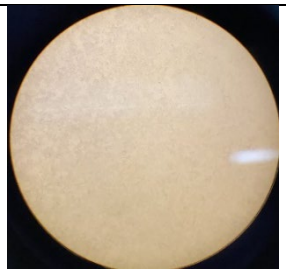		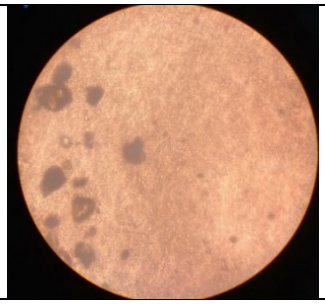	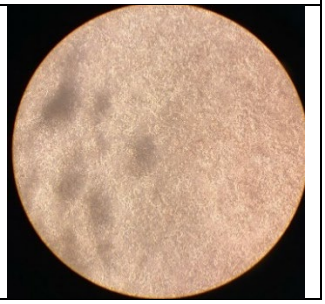

Table 3. Treatment assay and controls results from day 0. Images of the NIH3T3 seeded 3D collagen and HaCaT top monolayer seed two days after 10-minute 365nm UV exposure and vitamin application. Imaging both the lower and upper most sections of the collagen model at 100x, including after removing and/or

replacing the media containing the test vitamin.

The vitamin C treatment of the UV exposed models after two days was found to have completely dissolved the collagen of the model, rendering an overly confluent pool of cells at the bottom of the well, as seen by the image in Table 3 'Bottom Layer Old Media'. After having removed the media from this well, the image to the right of the aforementioned image, under 'Bottom Layer New/No Media', displays the monolayer of cell that had successfully adhered to the bottom of the well.

Effects on Cell Proliferation

Fluorescence Reading of Resazurin Assay (RFUs)		
UV Exposure and Treatments Applied	**Initial**	**2 Days Post**
No exposure	3,162,644	2,792,477
UV exposure	1,992,408	2,726,706
UV exposure + Vitamin E	-	2,591,105
UV exposure + Vitamin C	-	101,421
UV exposure + Vitamin B3	-	2,559,341

Table 4. Fluorescence readings at 530/590nm, measured in RFUs for each of the well conditions and done initially and 2 days after 10-minute 365 nm UV exposure.

Without exposure to UV light, the cell count measured via the resazurin assay was 3,162,644 RFUs at the start of the time course. After this reading, the reagent was added to the same well to get the 2,792,477 RFU measurement two days later. Directly after ten minutes of UV exposure, the assay was started on one of the models without vitamin treatment, yielding a measurement of 1,992,408 RFUs. A third model with 10-minute UV exposure, without vitamin treatment, was allowed to sit for two days before the Alamar Blue reagent was added, yielding a measurement of 2,726,706 RFUs. All vitamin-treated models were allowed to sit for two days after UV exposure before the reagent was added, resulting in values of 2,591,105 RFUs, 101,421 RFUs, and 2,559,341 RFUs for vitamins E, C, and B3, respectively.

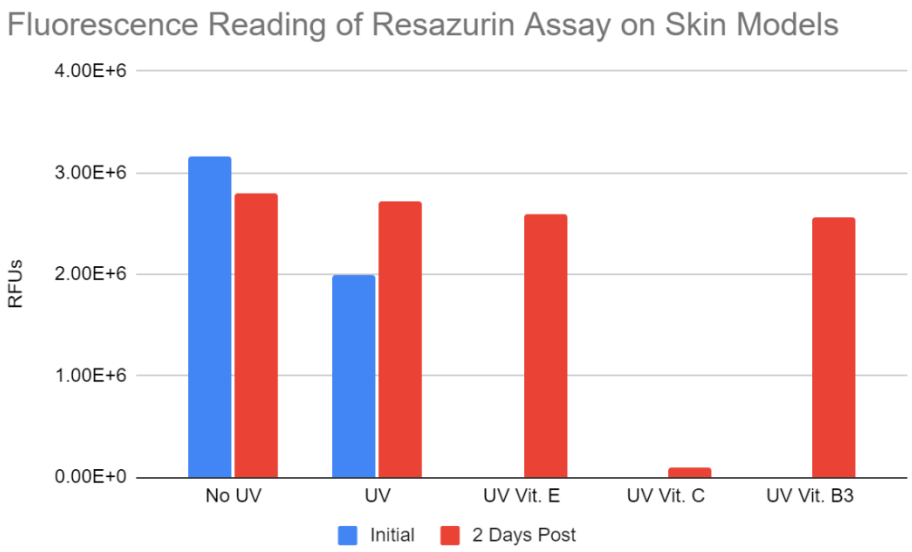

Figure 4. Fluorescence readings of the resazurin assay at 530/590nm measured in RFUs, organized by treatment type and time of measurement.

Viewing the RFU data from Table 4 in graphical form, the skin model not exposed to the 10-minute 365nm UV treatment was found to initially have the highest RFU reading of all the other models but decreased after two days of exposure; this two day post RFU reading, however, remained higher than the other UV exposed models. In terms of the UV exposed models, the initial RFU reading of the non-vitamin treated models was found to be lower than the model read two days after UV exposure, to a greater degree than the difference between the non-UV treated model reads. The UV exposed models treated with vitamin E and B3 were found to have slightly lower RFU reads than the two day post reads from both the no UV and UV exposed models. The UV exposed model treated with vitamin C was found to have the lowest RFU read, two days after exposure, of all the models by a large margin.

Effects on ROS Levels

Fluorescence Readings of ROS Assay (RFUs)		
UV Exposure and Treatments Applied	**Initial**	**2 Days Post**
No exposure	1271	4170
UV exposure	2115	1982
UV exposure + Vitamin E	-	1181
UV exposure + Vitamin C	-	3295
UV exposure + Vitamin B3	-	885

Table 5. Fluorescence readings at 485/535nm, measured in RFUs for each of the well conditions and done initially and 2 days after 10-minute 365nm UV exposure.

Without exposure to UV light, the ROS level measured via the resazurin assay was 1271 RFUs at the start of the time course. After this reading, reagent was added to the same well to get the 4170 RFU measurement two days later. Directly after 10-minute UV exposure, the reagent was added to one of the models, yielding a measurement of 2115 RFUs. A third model with 10-minute UV exposure, without vitamin treatment, was allowed to sit for two days before the ROS reagent was added it, yielding a measurement of 1982 RFUs. All vitamin-treated models were allowed to sit for two days after 10-minute UV treatment before the assay was started, resulting in values of 1181 RFUs, 3295 RFUs, and 885 RFUs for vitamins E, C, and B3, respectively.

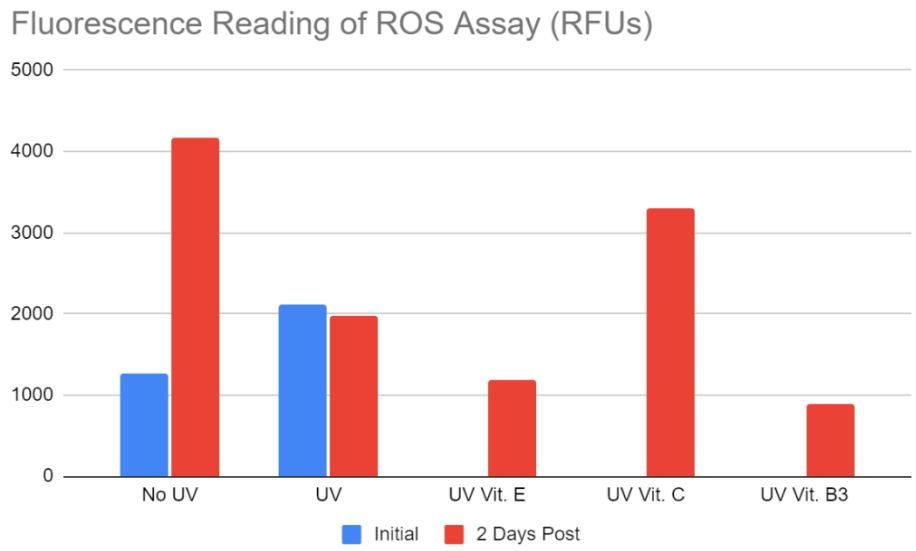

Figure 5. Fluorescence readings of the ROS assay measured in RFUs, organized by treatment type and time of measurement.

In graphical form, the ROS measurements show the no UV exposure led to a lower starting ROS reading, but a higher ROS reading after two days. Ten minutes of UV exposure led to roughly equivalent ROS readings directly after exposure and two days after exposure. Models treated with vitamins E and B3 had slightly lower ROS readings than the initial model that was measured without UV exposure. The model treated with vitamin C had a higher final ROS reading than the untreated model which had been exposed to UV, but a lower ROS reading than the untreated model that was not exposed to UV.

DISCUSSION

In the United States, skin cancer is one of the most common types of cancer that patients are diagnosed with. It is so common that an estimated 9,500 people are diagnosed every day. It has been shown that UV exposure is a major risk factor for many common types of skin cancer like melanoma [14]. Previously described in the *Introduction*, UV exposure can cause reactive oxygen species, or ROS, to be produced. ROS are harmful to cells as they can damage cell membranes and their DNA. Because of this, it is crucial to understand how antioxidant skin treatments affect ROS levels in skin after UV exposure. The data collected from these experiments show how the levels of ROS and cell proliferation rates are affected by antioxidant treatments after UV exposure on HaCaT and NIH-3T3 cells.

There are many limitations this study is constrained by. The model itself is very imperfect, as it does not accurately reflect the thickness of the layers of skin it is meant to represent. Additionally, the reagent used to measure ROS levels was not new, the age was unknown. This potentially impacted the measurements recorded and the amount of time necessary to see a non-background fluorescence reading. The integrated nature of this model is also not conducive to measuring the ROS and cell proliferation of the top and bottom layers, since they could not be separated and measured as their own separate entities. We can only make inferences based on the appearances of the top and bottom layers, limiting the conclusiveness of any potential findings regarding penetrative

effects of both irradiation and vitamin treatment. Vitamins E and B3 did not dissolve properly in media either, meaning that the actual concentration that the cells interacted with and were exposed to is unknown. Vitamin E was in the form of an oil, so it floated above the cells in the collagen model, and vitamin B3 was in the form of a powder which was not very soluble in media, so we cannot be certain about how much was intermingling with cells in the model.

When comparing the initial RFU readings of the non-irradiated models in both **Figure 4** and **Figure 5**, it is clear that increased ROS levels results in a lower cell count. However, it may be more drastic than these figures would seem to indicate. The non-irradiated models had, in both cases, been applied their respective assays on the same model for both the initial and 2 day post readings – in contrast to all the other models that had a separate model for the two time points. This is important to note as the ROS assay required the cells in the collagen models to be without media for the established incubation time, potentially causing mass cell death, as a result of ROS creation, by the time the 2 day post read was conducted. While the resazurin assay did not require the removal of the media during the incubation time, it is similarly possible that this incubation with the Alamar Blue reagent caused some cell death, either directly or indirectly, by the formation of ROS. Unfortunately, this makes drawing conclusions from this data less reliable, since the baseline measurement was under conditions which were different from the rest of the models.

The vitamin E and B3 treatment had significantly lower ROS levels in comparison to the 2 days post measurement of all other models. This, in reference to the high ROS levels in the vitamin C treatment, is most likely due to the high acidity of vitamin C. It was acidic enough to dissolve the collagen in the models it was treating, and therefore likely killed many of the cells in the model. This mass cell death would have led to the release of intracellular metabolic components, some of which are ROS, leading to higher ROS levels being observed. It cannot be directly concluded that the ROS killed the cells in the vitamin C model because most of the cells were removed when the media, along with the dissolved collagen, was aspirated from the well. This removed any unbound cells from the model, as seen in **Figure 4**. However, when compared to the models which weren't treated with any vitamins, the E and B3 treated models clearly had lower ROS levels, proving that the vitamins were effective at lowering ROS levels in a collagen matrix.

While it is very difficult to draw conclusions from the data gathered from this experiment, an attempt to speculate as to the relationship of the vitamin treatment, ROS levels, and cell counts will be made based on **Figures 4 and 5**. As mentioned previously, the treatments with vitamin E and B3 do appear to decrease ROS levels relative to the 2 day post UV exposure untreated models. While this would theoretically result in higher cell counts if the ROS were the only cause of cell death/decreased viability, this is not what is seen based on **Figure 4** where the untreated UV model 2 days post was found to have slightly higher cell counts than those treated with vitamin E and B3. This could indicate that, while those vitamin treatments are decreasing ROS levels, the vitamins themselves could also be altering the environmental conditions of the models in a manner that decreases cell viability. This is supported further by the vitamin c treated models as it saw a huge reduction in cell count, possibly due to the collagen dissolving effects demonstrated by the images of **Table 3**.

CONCLUSIONS

The most conclusive assessment that this study supports is that vitamins E and B3 are effective antioxidants, reducing ROS levels to around or below the levels present in the initial measurement. Additionally, this study also concludes that increased ROS levels do negatively affect the cell viability of NIH 3T3 and HaCaT cells. In terms of the generation of ROS, this study concludes that, at least initially, UV irradiation of a collagen skin model using NIH 3T3 and HaCaT cells increases ROS levels. The intensity of UV radiation in this ROS generation appears to be negatively affected as it passes through a cell seeded 3D collagen model.

As this paper shows topical antioxidant treatments do have an effect on lowering ROS levels, it would be beneficial to continue and expand this study. One aspect that could be improved upon in a future study would be the number of models used. If duplicates or triplicates were created for each condition, more conclusions could be drawn from the results collected. Concentrations of vitamins, vitamin C specifically, should be adjusted to ensure the stability of the models during treatment.

ACKNOWLEDGMENTS

The authors thank the lab instructor, Lou Roberts, and the two lab assistants, Vanesa Lopa and Shruti Shastry, for their excellent help in the formation and execution of this experiment and the feedback on this paper.

REFERENCES

1. Skin Cancer Facts & Statistics. (n.d.). *The Skin Cancer Foundation*. Retrieved February 28, 2024, from https://www.skincancer.org/skin-cancer-information/skin-cancer-facts/

2. Shields, H. J., Traa, A., & Van Raamsdonk, J. M. (2021). Beneficial and Detrimental Effects of Reactive Oxygen Species on Lifespan: A Comprehensive Review of Comparative and Experimental Studies. *Frontiers in Cell and Developmental Biology*, *9*. https://www.frontiersin.org/articles/10.3389/fcell.2021.628157

3. de Jager, T. L., Cockrell, A. E., & Du Plessis, S. S. (2017). Ultraviolet Light Induced Generation of Reactive Oxygen Species. In S. I. Ahmad (Ed.), *Ultraviolet Light in Human Health, Diseases and Environment* (pp. 15–23). Springer International Publishing. https://doi.org/10.1007/978-3-319-56017-5_2

4. Pisoschi, A. M., Pop, A., Iordache, F., Stanca, L., Predoi, G., & Serban, A. I. (2021). Oxidative stress mitigation by antioxidants—An overview on their chemistry and influences on health status. *European Journal of Medicinal Chemistry*, *209*, 112891. https://doi.org/10.1016/j.ejmech.2020.112891

5. Ganji, S. H., Qin, S., Zhang, L., Kamanna, V. S., & Kashyap, M. L. (2009). Niacin inhibits vascular oxidative stress, redox-sensitive genes, and monocyte adhesion to human aortic endothelial cells. *Atherosclerosis*, *202*(1), 68–75. https://doi.org/10.1016/j.atherosclerosis.2008.04.044

6. Colombo, I., Sangiovanni, E., Maggio, R., Mattozzi, C., Zava, S., Corbett, Y., Fumagalli, M., Carlino, C., Corsetto, P. A., Scaccabarozzi, D., Calvieri, S., Gismondi, A., Taramelli, D., & Dell'Agli, M. (2017). HaCaT Cells as a Reliable In Vitro Differentiation Model to Dissect the Inflammatory/Repair Response of Human Keratinocytes. *Mediators of Inflammation*, *2017*, 7435621. https://doi.org/10.1155/2017/7435621

7. *NIH3T3 Cells*. (n.d.). NIH 3T3 CELL LINE. Retrieved February 28, 2024, from https://nih3t3.com/

8. *Cells | Free Full-Text | Heterogeneity of the NIH3T3 Fibroblast Cell Line*. (n.d.). Retrieved February 28, 2024, from https://www.mdpi.com/2073-4409/11/17/2677

9. Yousef, H., Alhajj, M., & Sharma, S. (2024). Anatomy, Skin (Integument), Epidermis. In *StatPearls*. StatPearls Publishing. http://www.ncbi.nlm.nih.gov/books/NBK470464/

10. *Collagen solution from bovine skin* -. (n.d.). Retrieved February 28, 2024, from https://www.sigmaaldrich.com/US/en/substance/collagensolutionfrombovineskin1234598765

11. Antoine, E. E., Vlachos, P. P., & Rylander, M. N. (2014). Review of Collagen I Hydrogels for Bioengineered Tissue Microenvironments: Characterization of Mechanics, Structure, and Transport. *Tissue Engineering Part B: Reviews*, *20*(6), 683–696. https://doi.org/10.1089/ten.teb.2014.0086

12. Poonawalla, T., & Diven, D. (2008). *Anatomy of the Skin*. Utmb. https://www.utmb.edu/pedi_ed/CoreV2/Dermatology/page_03.htm

13. Qu, Z., Chen, Y., Du, K., Qiao, J., Chen, L., Chen, J., & Wei, L. (2024). ALA-PDT promotes the death and contractile capacity of hypertrophic scar fibroblasts through inhibiting the TGF-β1/Smad2/3/4 signaling pathway. *Photodiagnosis and Photodynamic Therapy*, *45*, 103915. https://doi.org/10.1016/j.pdpdt.2023.103915

14. Skin cancer (2022). American Academy of *Dermatology Association*. Retrieved March 1, 2024, from https://www.aad.org/media/stats-skin-cancer#:~:text=Skin%20cancer%20is%20the%20most%20common%20cancer%20in%20the%20United%20States.&text=Current%20estimates%20are%20that%20one,skin%20cancer%20in%20their%20lifetime.&text=It%20is%20estimated%20that%20approximately,with%20skin%20cancer%20every%20day